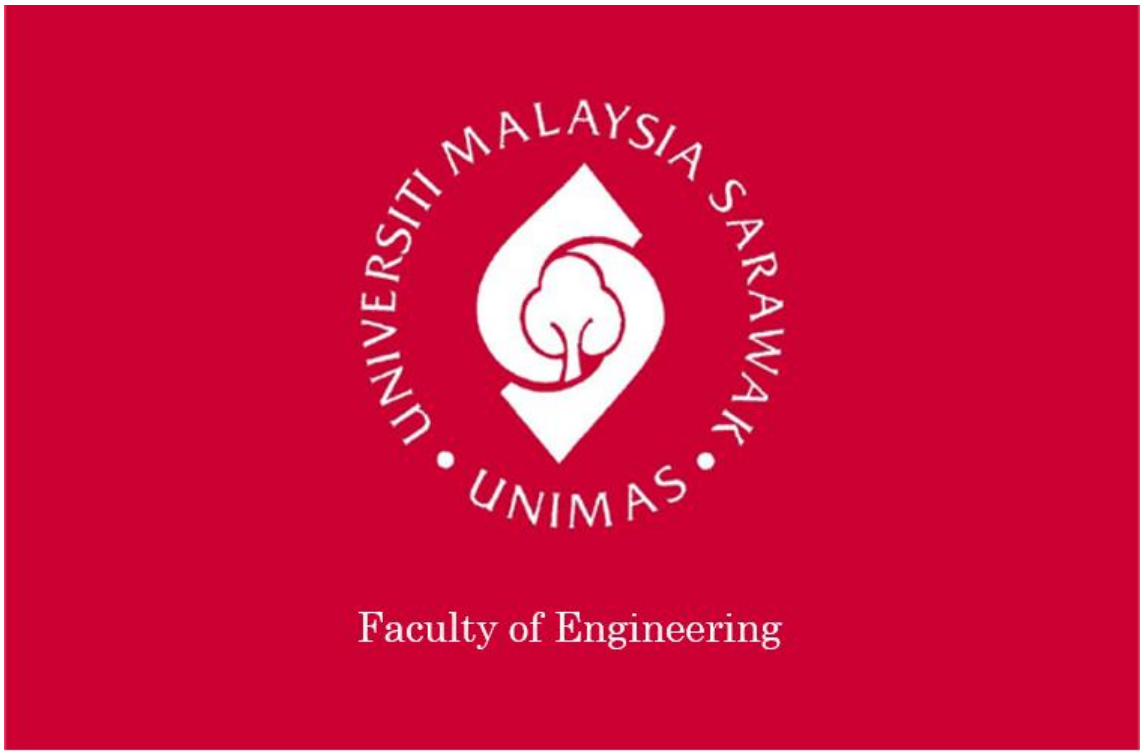

HEAVY METAL REMOVAL USING MIXED MATRIX MEMBRANE INCORPORATED WITH MONTMORILLONITE

JUSTINA LUISA ANAK JANIS

Bachelor of Engineering with Honours

(Chemical Engineering)

2022

UNIVERISITI MALAYSIA SARAWAK

Grade: _____
Please tick (/)
Final Year Project Report (/)
Masters ( )
PhD ( )

DECLARATION OF ORIGINAL WORK

This declaration is made on the **Declaration Date**

Student's Declaration:

I, **JUSTINA LUISA ANAK JANIS (64809)**, DEPARTMENT OF CHEMICAL ENGINEERING AND ENERGY SUSTAINABILITY, FACULTY OF ENGINEERING, hereby declare that the work entitled **HEAVY METAL REMOVAL USING MIXED MATRIX MEMBRANE INCORPORATED WITH MONTMORILLONITE** is my original work. I have not copied from any other student's work or from any other sources except where due reference or acknowledgement is made explicitly in the text, nor has any part been written for me by another person.

3/7/2022
…… ……..
Submission Date Name: JUSTINA LUISA ANAK JANIS
Matrix Number: 64809

Supervisor Declaration

I **MOHAMED AFIZAL BIN MOHAMED AMIN** hereby certifies that the work entitled **HEAVY METAL REMOVAL USING MIXED MATRIX MEMBRANE INCORPORATED WITH MONTMORILLONITE** was prepared by the above-named student and was submitted to the "FACULTY" as a partial/full fulfillment for the conferment of BACHELOR OF ENGINEERING WITH HONOURS (CHEMICAL ENGINEERING) and the aforementioned work to the best of my knowledge, is the said students' work.

Received for examination by Date:

…….. …….
Name: Declaration Date

I declare this Report is classified as (Please tick (√)):

	CONFIDENCIAL	(Contains confidential information under the Official Secret Act 1972) *
	RESTRICTED	(Contains restricted information as specified by the organization where research is done)
√	**OPEN ACCESS**	

Validation of Report

We therefore duly affirmed with free consent and willingness declared that this said Report shall be placed officially in Department of Chemical Engineering and Energy Sustainability with the abide interest and right as follows:

- This Report is the sole legal property of Department of Chemical Engineering and Energy Sustainability, Universiti Malaysia Sarawak (UNIMAS).
- The Department of Chemical Engineering and Energy Sustainability has the lawful right to make copies for the purpose of academic and research only and not for other purposes.
- The Department of Chemical Engineering and Energy Sustainability has the lawful right to digitize the content to for the Local Content Database.
- The Department of Chemical Engineering and Energy Sustainability has the lawful right to make copies of the Report for academic exchange between Higher Learning Institute.
- No dispute or any claim shall arise from the student itself neither third party on this Report once it becomes sole property of The Department of Chemical Engineering and Energy Sustainability, Universiti Malaysia Sarawak (UNIMAS).
- This Report or any other material, data and information related to it shall not be distributed, published or disclosed to any party by the student except with The Department of Chemical Engineering and Energy Sustainability, Universiti Malaysia Sarawak (UNIMAS) permission.

Student's signature: _____ Date: 3/7/2022	Supervisor's signature: _____ Date: 3/7/2022

Current Address:
DEPARTMENT OF CHEMICAL ENGINEERING AND ENERGY SUTAINABILITY, FACULTY OF ENGINEERING, 94300 KOTA SAMARAHAN SARAWAK.

Notes: *If the Report is **CONFIDENTIAL** or **RESTRICTED**, please attach together as annexure a letter from the organization with the period and reasons for confidentially and restriction.

APPROVAL SHEET

This final year project thesis, which entitles **"HEAVY METAL REMOVAL USING MIXED MATRIX MEMBRANE INCORPORATED WITH MONTMORILLONITE"** was prepared by **JUSTINA LUISA ANAK JANIS (64809)** as a partial fulfillment for the Bachelor of Engineering with Honours (Chemical Engineering) is hereby read and approved by:

3/7/2022

Name: MOHAMED AFIZAL BIN MOHAMED AMIN

Date

(Supervisor)

HEAVY METAL REMOVAL USING MIXED MATRIX MEMBRANE INCORPORATED WITH MONTMORILLONITE

JUSTINA LUISA ANAK JANIS

A dissertation submitted in partial fulfilment

of the requirement for the degree of

Bachelor of Engineering with Honours

(Chemical Engineering)

Faculty of Engineering

Universiti Malaysia Sarawak

2022

ACKNOWLEDGEMENT

The author would like to dedicate sincere gratitude to her supervisor, Mr. Mohamed Afizal bin Mohamed Amin for his counsel, knowledge, and continuous guidance towards the thesis completion. Besides, the author would like to thank the lecturers and staff of the Chemical Engineering Department for their contributions to the sharing of ideas. Last but not least, a special thanks goes out to her beloved family and friends for their love, support, and motivation during the completion final year project.

ABSTRACT

The removal of heavy metal by using mixed matrix membrane (MMM) incorporated with montmorillonite (MMT) was studied. In general, MMM referred to membrane that consists of polymers filled with inorganic material in order to enhance the membrane's chemical and physical properties particularly in water separation application. In this study, MMM was prepared using polysulfone (PSf) polymer incorporated with MMT and casted using phase inversion technique. The prepared membrane were characterized using Fourier Transform Infrared (FTIR) to analyze the functional groups, Scanning Electron Microscopy-Energy Dispersive X-ray (SEM-EDX) to observe the membrane cross section morphology and conduct elemental analysis, and water uptake analysis to know the membrane capability to absorb water. Then, the performance of prepared membranes were evaluated in terms pure water flux and capability of the membrane to remove heavy metal in wastewater. Based on the membrane performance, 1.0MMM was the most preferred as it has significant rejection of cadmium and lead as well as high pure water flux, surface porosity and permeate flux.

Keywords: *mixed matrix membrane, montmorillonite (MMT), heavy metal removal.*

ABSTRAK

Penyingkiran logam berat dengan menggunakan membran matriks campuran (MMM) yang digabungkan dengan montmorilonit (MMT) telah dikaji. Secara umum, MMM merujuk kepada membran yang terdiri daripada polimer yang diisi dengan bahan anorganik untuk meningkatkan sifat kimia dan fizikal membran terutama dalam aplikasi pemisahan air. Dalam kajian ini, MMM akan disiapkan menggunakan polimer polisulfon (PSf) yang digabungkan dengan MMT dan dilemparkan menggunakan teknik penyongsangan fasa. Membran yang disediakan dicirikan menggunakan Inframerah Fourier Transformasi (FTIR) untuk menganalisis kumpulan berfungsi, Mengimbas Mikroskopi Elektron-Sinar Penyebaran Tenaga (SEM-EDX) untuk memerhatikan morfologi keratan rentas membran dan melakukan analisis unsur, dan analisis pengambilan air untuk mengetahui kemampuan membran untuk menyerap air. Akhir sekali, prestasi membran yang disiapkan dinilai dari segi aliran air tulen dan keupayaan membran untuk membuang logam berat dalam air sisa. Berdasarkan prestasi membran, 1.0MMM adalah yang paling dikehendaki kerana mempunyai penolakan kadmium dan plumbum yang ketara serta mempunyai fluks air tulen, keliangan permukaan dan fluks meresap yang tinggi.

Kata kunci: *membrane matriks campuran, montmorilonit, penyingkiran logam berat.*

TABLE OF CONTENTS

LIST OF TABLES

LIST OF FIGURES

CHAPTER 1

INTRODUCTION

1.1 Background of study

Nowadays, water was regarded as one of the basic necessities required for urbanization and industrialization. Water was necessary for the development of cities since it is required for residents' drinking and sanitation needs in order to build and maintain a healthy environment. On the other hand, water was used in the industrialization process for a variety of purposes, including heating, cooling, dilution, and many more. Nonetheless, a growing problem arises when wastewater was not properly treated, resulting in water pollution. There were several water pollutants that present in water bodies such as nutrients, halogen, heavy metals, organic pollutants, and microbial pollutants (Madhav *et al*., 2020). The focus of this research project was on water pollutants, specifically heavy metals. Heavy metals were one of the toxic and hazardous substances that, when present in high concentrations, pose a concern to human health. According to Qasem *et al*., heavy metals were considered as non-biodegradable material. Non-biodegradable materials remain in water bodies for a long period of time because they were resistant to microbial and chemical degradation (Qasem *et al*., 2021). Moreover, heavy metals were highly soluble in water. Hence, heavy metals accumulated in food chains, providing major health concerns to living organisms that consume water with high heavy metal concentrations. Based on the study by Muharrem & Ince, heavy metals were primarily found in wastewater from modern industrial sources such as mining, metal processing factories, protective coatings, chemical manufacturing, electrolysis, tannery, metalworking, fuel source, pulp, and the manufacture of various polymers (Muharrem & Ince, 2017). As a result, heavy metal processing industries play an important role in treating heavy metals before discharging them into water bodies.

Most manufacturing operations generate wastewater as an inevitable by-product. It was critical to have effective wastewater treatment so that freshwater resources and water supply

can be augmented and made available to living organisms. This also helps to alleviate water scarcity. As stated by Crini & Lichtfouse, flotation, precipitation, oxidation, solvent extraction, evaporation, carbon adsorption, ion exchange, membrane filtration, electrochemistry, biodegradation, and phytoremediation are some of the technologies used in wastewater treatment (Crini & Lichtfouse, 2019). Membrane materials can be classed as organic, inorganic, or a combination of both. Organic membranes were created from synthetic organic polymers meanwhile inorganic membranes are usually from ceramics, metals, clay minerals, zeolites or silica (Obotey Ezugbe & Rathilal, 2020). Membrane technology in wastewater treatment had various advantages, including low capital cost, reduced equipment size, low energy requirements, minimal chemical usage, easy accessibility, and environmental friendliness. Hence, membrane technology has lately been demonstrated as a more viable option in wastewater treatment.

Organic membranes, commonly known as polymeric membranes were extensively used in the water separation field because they are cost-effective and versatile. These membranes can be customised to meet the unique requirements of the process in which they were utilised. Thus, selective separation was possible when utilizing the polymeric membranes. Based on the literature of Sonawane *et al*., the most significant property required in polymeric membranes was affinity for a certain component (Sonawane *et al*., 2021). A suitable selection of polymeric membrane for a certain function is critical. This was because the polymer must have the right affinity and be able to tolerate the separation environment (Dickhout *et al.*, 2017). Some examples of polymeric membranes were polysulfone (PSf), polyethersulfone (PES), cellulose acetate (CA), polyvinylidene fluoride (PVDF) and many more. A various characteristics including dense and porous polymeric membranes can be executed depending on the requirement. It was also trivial to regulate the pore size of polymeric membranes during their synthesis (Sonawane *et al*., 2021). This indicates that polymeric membranes were highly flexible, and that the polymeric membranes may be synthesised in a small amount of space. According to Ladewig & Al-Shaeli, the key advantages of polymeric membranes were their ease of preparation, low cost, lower energy requirements, flexibility in membrane layout, and relatively low working temperature, which is also connected with less rigorous material requirements in module assembly (Ladewig & Al-Shaeli, 2017). Therefore, the application of polymeric membranes can be employed for the removal of heavy metal in water separation mechanism.

Montmorillonite (MMT) belongs to smectite group that was one of the most commonly used clay minerals. It derives from the 2:1 clay layer structural family, which consists of two fused siloxane tetrahedral sheets that share edges with an octahedral sheet in the middle (Bee *et al*., 2018). The octahedral sheet was made from either aluminium or magnesium hydroxide. According to Liu *et al*., MMT was obtained through mineralization of ores in which warm and humid environments are the main factors of the process (Liu *et al*., 2019). MMT can be employed as a pollutants natural scavenger through isomorphic substitution. Processes such as ion exchange, adsorption, dispersion, expansibility, and suspension were used in isomorphic substitution to uptake cations and anions (Liu *et al*., 2021). In general, negative layer charges of magnesium ions and aluminium ions were obtained in the alumina octahedral and silicon tetrahedral respectively, results from the isomorphic substitution. The negative layer charges of magnesium ions are for aluminium ions meanwhile the negative layer charges of aluminium ions are for silicon ions. Due to the presence of numerous active sites including Bronsted and Lewis acid sites on MMT's surfaces, MMT was known to be a good adsorbents. To maintain the equilibrium of metal ions between the layers, certain substitutable cations can be exchanged by other cations. Aside from that, the Van der Waals force and electrostatic force connect the MMT interlayer to the nanosheets that hold the MMT particles together. Lastly, because of its low cost, non-hazardous, and vast deposits, MMT was particularly appealing as an inorganic membrane.

1.2 Problem statement

Membrane fouling was one of the most significant issues associated to the usage of polymeric membranes in wastewater treatment. This was owing to the hydrophobic nature of the polymeric membrane, which allows foulants to adhere to the membrane's surface. Based on the literature of AlSawaftah *et al*., the membrane foulants include particulate, organic, inorganic, and biological microorganisms (AlSawaftah *et al*., 2021). Consequently, membrane fouling cause a reduction of membrane water flux (Hebbar *et al*., 2018). Membrane water flux refers to the total water flow across the membrane. As the membrane's surface was blocked by the deposition of foulants, only a limited amount of water may pass through the membrane. This results in increasing of operational cost and the lifespan of the polymeric membrane is reduced. To address this problem, the fabrication of a polymeric membrane with the

hydrophilic nature of an inorganic membrane is required to improve the polymeric membrane's performance.

Aside from that, polymeric membrane had a trade-off relationship between permeability and selectivity. In general, permeability relates to the rate at which water passes through a membrane, whereas selectivity refers to the degree to which heavy metals were rejected from water. The capital cost of the polymeric membrane was decreased when higher permeability was obtained. This was because the amount of membrane area required to treat heavy metals in water is reduced. Conversely, higher selectivity results in higher purity of water as the membrane was impermeable to heavy metals and separates them from the water. High permeability and selectivity polymeric membranes were desirable. Nevertheless, more permeable polymeric membranes were usually found to be less selective, and vice versa (Cheng *et al*., 2018). This was attributable to the porous membranes' wide distribution of pores and the nonspecific interactions of heavy metals with polymeric membranes. According to Kheirieh *et al*., porosity and hydrophilicity were the most essential parameters that determine the permeability capabilities of polymeric membrane (Kheirieh *et al*., 2018). The permeability of the polymeric membrane increased as the broad distribution of pores in the porous membrane grows, but the selectivity of heavy metals decreased. Therefore, MMT was a viable option to increase the number of small surface pores in the membrane.

As for inorganic membranes, these membranes plays an essential role in the membrane technology evolution. Unfortunately, inorganic membranes had a number of disadvantages, including brittleness, high production costs, a complicated fabrication technique, and difficulty scaling up, as reported by Vinoba *et al.* (Vinoba *et al*., 2017). Moreover, Qadir *et al*. stated that despite the fact that a large and new number of inorganic membranes had been researched in the literature, they had yet to achieve popularity due to a variety of factors such as expensive or the high cost of the synthesis process (Qadir *et al*., 2017). Therefore, critical studies and understanding of the inorganic membrane's chemical and physical properties, stability, as well as the compatibility factor, were required before they can be successfully implemented in membrane technology, particularly for the removal of heavy metals. Successful implementation of inorganic membrane in water separation mechanism aids in obtaining high selectivity of heavy metals in water. Finally, suitable inorganic membranes must be considered so that heavy metals can be properly removed in wastewater treatment.

1.3 Research Questions

This research project will focus on the study of heavy metal removal by embedding MMT into polymeric membrane via phase inversion approach. Therefore, the research questions of this project are:

a) What is the significant effect of the membrane surface modification with MMT via phase inversion approach?
b) How will the chemical properties and morphology influenced the prepared membrane?
c) What is the efficiency of the prepared membrane on heavy metal removal capability?

1.4 Objectives

The objectives of this study are as follows:

a) To fabricate polymeric membrane with MMT at different loading via phase inversion technique.
b) To characterize the MMT and the prepared membrane.
c) To analyze performance of the prepared membrane on pure water permeability and analyze the capability on heavy metal removal in wastewater.

1.5 Scopes of study

The following are the scopes of study that have been identified:

For Objective 1:

a) Prepare a flat sheet polysulfone (PSf) polymeric membrane via phase inversion method.
b) Modify the flat sheet polymeric membrane surface with additional of MMT using three different concentrations by using phase inversion technique.

For Objective 2:

a) Characterize the MMT using PSA to analyze the particle size distribution, FTIR to evaluate the functional groups, SEM to determine the morphology and BET to investigate porosity and surface area.
b) Study the characteristics of the prepared membrane using FTIR, SEM-Energy Dispersive X-ray (EDX) to evaluate morphology along with elemental composition, BET and water uptake analysis.

For Objective 3:

a) Evaluate the effects of MMT loading parameters on water permeability.
b) Assess the heavy metal removal capability at different concentration of MMT.

1.6 Summary

In this chapter, the background of study for heavy metals, wastewater treatment via membrane technology, polymeric membrane, and MMT are presented. Besides, the issues regarding the utilisation of polymeric membrane as well as inorganic membrane are also discussed. Finally, the research questions, objectives, scopes of study and expected results are considered.

CHAPTER 2

LITERATURE REVIEW

2.1 Heavy metals

Heavy metals are generated from human sources in a variety of sectors, including agriculture, industry, home sewage, and others, and have thus become a hazard to human health and the environment. Following that, they had the most direct impact on the environment, with marine ecosystem degradation, soil deterioration, and heavy metals entering the food chain through plants, producing severe consequences on humans and animals. This is owing to its properties, which include being extremely soluble, stable, and non-biodegradable, as well as the ability to travel across aqueous medium without being digested by the body, resulting in buildup in soft tissues (Chai *et al*., 2021). Furthermore, Zuo *et al*. reported that heavy metal contamination is becoming more widely recognised as a severe global environmental problem, owing to its high toxicity, non-biodegradability, and bioaccumulation, all of which pose serious threats to human health and ecosystem stability (Zuo *et al*., 2021). This research study focuses on cadmium and lead as the heavy metals since they were considered as one of the most toxic and widespread elements in water bodies.

2.1.1 Cadmium

The regulatory limit of cadmium in drinking water was 0.005 ppm (Azimi *et al*., 2017). As for wastewater, the cadmium allowable limit was 0.003 ppm as mentioned by Kinuthia *et al*. (Kinuthia *et al*., 2020). As cadmium was exposed above the allowable limit, kidney damage was one of the most prominent potential health effects resulted from the exposure (Dutta *et al.*, 2021). Besides, cadmium had chronic toxicity towards children including body system damage and cancers of internal organ which may be due to the consumption of contaminated food or surrounded by the environment, workplace or industries that containing cadmium in the

waterways (Kinuthia *et al*., 2020). Lastly, the particle size of cadmium was ranging from 0.05μm to 0.1μm based on the study of Vadgama *et al*. (Vadgama *et al*., 2017).

2.1.2 Lead

As for lead, the regulatory limit in drinking water was 0.015 ppm (Azimi *et al*., 2017). On the other hand, 0.01 ppm was the allowable limit for lead in wastewater as reported by Kinuthia *et al*. (Kinuthia *et al*., 2020). High concentration of lead can cause serious health issues such as gastrointestinal, neurological, hematological, cardiovascular, and renal problems when excessive amounts of lead were exposed to human being (Dutta *et al*., 2021). Aside from that, Kinuthia *et al*. studied that high concentration of lead threats human health such as anaemia and deterioration in synthesizing haemoglobin, thus having headache, dullness, and memory loss as initial symptoms (Kinuthia *et al*., 2020). Moreover, lead toxicity in excess of the permitted limit causes inferior intelligence ability in children (Kinuthia *et al*., 2020). Finally, the particle size of lead was within 1μm as stated by Matthew & Krishnamurthy (Matthew & Krishnamurthy, 2018).

The particle size of contaminants were one of the most essential parameters in membrane filtration technology. This was because the contaminant's size contributes to the development of the membrane mechanism needed to remove heavy metals from water. For instance, if the size of cadmium and lead were smaller than the pore size of the membrane, the heavy metals will easily pass through the pore of the membrane, thereby causing an incomplete membrane separation process. As a result, in-depth research into heavy metal removal, including the consequences, allowable limit, and particle size, are required in order for the membrane separation mechanism to function entirely and properly.

2.2 Membrane for water separation

The membrane separation mechanism for water separation in this study was based on water filtration module. According to Judd, the technology of membrane had been developed

since in the mid-19th century in the application of water treatment which includes the UF separation using bovine heart-based, synthetic UF, MF, RO membrane (Judd, 2017),. Each membrane mechanism had its own set of characteristics, such as pore size and the operating parameters that must be met when using them. It was discovered that the pore size of the membrane affects the rejection of pollutants using membrane technology, thereby a suitable type of membrane mechanism must be chosen to achieve maximum contaminant rejection. Subsequently, an in-depth evaluation of membrane filtration mechanisms including microfiltration (MF), ultrafiltration (UF), nanofiltration (NF), and reverse osmosis (RO) membrane are presented.

First and foremost, MF membrane had pore sizes ranging from 0.1 μm to 10 μm and operating pressure within 1 bar to 6.2 bar, as reported by Maddah *et al*. (Maddah *et al*., 2018). It was able to remove suspended matter, zooplankton, algae, bacteria, and protein aggregates (Abetz *et al*., 2021). Despite its removal capabilities, the MF membrane had two main weaknesses which are it cannot entirely remove viruses and it cannot remove pollutants with a size of less than 1 mm. Since MF membrane was not an absolute virus barrier, it can be used in combination with disinfection to manage these microorganisms in water. In disinfection process, chlorination was one of the common steps in removing pathogens which leads to the addition of chemical substance. Aside from that, pollutants that have 1 mm in size or smaller than the pore size of the MF membrane will pass through the membrane easily. To conclude, MF membrane was employed to remove micrometer sized matter.

On the other hand, UF membrane was denser than MF membrane and widely used to remove some viruses, colloidal matter, macromolecules, proteins, and vitamins (Abetz *et al*., 2021). Based on the study of Maddah *et al*., it operated with pressure of 1 bar to 10 bar and has pore sizes within 1 nm to 100 nm (Maddah *et al*., 2018). It was discovered that there was no usage of chemicals required in UF membranes. In contrast, it possessed a simple automation in terms of size-exclusion filtration, consistent quality of treated water in terms of particle and microbial removal, process and plant compactness. However, Nqombolo *et al*. stated that UF membrane had certain disadvantages including inability to remove any dissolved inorganic pollutants from water and the need for routine cleaning to ensure high pressure water flow due to the membrane fouling phenomenon (Nqombolo *et al*., 2018). In summary, UF membrane was one of the pressure-driven membrane that removes pollutants with ultrafine porosity feature.

Apart from that, the other membrane technology namely NF membrane had denser and higher hydrodynamic resistance as compared to UF membrane, necessitating a larger driving force for filtration and used to separate small organic molecules and divalent salts (Asad *et al.*, 2020). In addition, Nqombolo *et al.* stated that the NF membrane can remove ions that contribute considerably to osmotic pressure, allowing for higher operation pressures (Nqombolo *et al.*, 2018). The loose selective thin film structure and small pore diameters of NF membranes were adequate and efficient for isolating metal salts (Abdullah *et al.*, 2019). NF membrane had pore sizes of 1 nm to 10 nm with operating pressure ranging from 20 bar to 40 bar (Maddah *et al*., 2018). In addition, the NF membrane can eliminate alkalinity and hardness from water. Since the NF membrane was capable of removing alkalinity from water, the resulting product water may be corrosive. To reduce water corrosivity, control techniques such as blending raw and product water or adding alkaline chemicals were required. Moreover, pre-treatment of hard water was necessary to avoid hardness ions from accumulating on the NF membrane that may reduce the performance of the membrane. In short, the NF membrane was a good membrane for removing contaminants from water that demands high operating parameters.

Last but not least, RO membrane was one of the pressure-driven membranes that were solely permeable to water molecules and were used to remove dissolved solids and smaller particles. It was categorized as nonporous membrane as it does not have definite pores and the membrane was denser than NF membrane that capable of isolating monovalent ions. The pore sizes for RO membrane was less than 1 nm and the range of operating pressure was from 30 bar to 100 bar (Maddah *et al*., 2018). The pressure delivered to the RO membrane must be sufficient to allow water to overcome the osmotic pressure. The net movement of water, according to the theoretical principle of osmosis, was from an area of low solute concentration to a region of high solute concentration. RO membrane operates in the reverse direction, forcing water molecules to travel against the concentration gradient by applying pressure (Abdullah *et al.*, 2019). Moreover, RO membrane had a significantly tighter pore structure than UF membranes, therefore they require less maintenance as it able to convert hard water to soft water and were essentially capable of eliminating all particles, bacteria, and organics. As stated by Nqombolo *et al.*, the utilization of high pressure, the fact that RO membrane was more expensive than other membrane technologies, and the fact that they are prone to fouling are all

negatives (Nqombolo *et al.*, 2018). To summarise, the RO membrane was a potential solution for effectively removing smaller particles like salts or ions.

2.3 Types of Membrane

Membranes can be classified as organic membrane, inorganic membrane and MMM. The in-depth understanding of most common used organic membranes such as cellulose acetate (CA), polyethersulfone (PES), polyvinylidene fluoride (PVDF) and polysulfone (PSf) were provided in this subtopic. As for inorganic membrane, the review of materials including ceramics, silica, zeolite and layer silicates clay mineral membranes were presented. Moreover, the evaluation of various types of layer silicates clay minerals such as kaolinite, smectite, and chlorite were discussed thoroughly. Lastly, the literature works regarding the fabrication of MMM was reviewed in terms of the type of organic and inorganic membrane, the membrane mechanisms, water flux, types of heavy metals with its concentration, removal capacity as well as advantages and disadvantages of the membrane.

2.3.1 Organic membrane

Organic membranes also referred as polymeric membranes were widely used for the application of lab and industry. Nowadays, polymeric membranes were the most frequently utilized membrane in water treatment and desalination technology. Organic membranes that were usually implemented in water separation processes such as cellulose acetate (CA), polyethersulfone (PES), polyvinylidene fluoride (PVDF) and polysulfone (PSf) were analysed critically.

Primarily, CA membrane had been found in most literature research as the commonly employed polymer in the fabrication of membrane. It can be used to prepare various types of membrane mechanism including MF, UF, NF, and RO membranes. Cellulose was the main component to derive CA and considered as biodegradable material that can be obtained from natural resources. Due to the insoluble nature of cellulose, other chemical compounds such as acetic anhydride and acetic acid were necessary in the manufacture of CA membrane. Apart

from the biodegradable and natural resources of CA membrane, it was determined that disadvantages including low chemical resistance, thermal resistance, and insufficient mechanical strength are associated to the CA usage (Dong *et al*., 2021). For these reasons, the use of specific chemicals is necessary to enhance the properties of CA membranes as well as modify the surface of CA membranes.

Besides, PES membrane was a type of polymeric membrane that had transparent and amorphous structure and was frequently utilised in the field of water separation. It has excellent properties in terms of oxidative, thermal, hydrolytic stability, and good mechanical property. Additionally, PES membrane was considered as an inert membrane that stable in water and resistant to several factors such as mechanical, thermal and chemical due to high triglycerides feature. PES was created chemically through a condensation reaction between bisphenol A and dichlorodiphenylsulfone, and it follows the mechanism of aromatic nucleophilic replacement, as studied by Alenazi *et al*. (Alenazi *et al*., 2017). Despite their widespread use, PES membranes had drawbacks. The membrane's main drawback was that it is relatively hydrophobic that cause membrane fouling. As a result, the current trend of combining PES membranes with other membrane materials was being explored to reduce fouling and improve biocompatibility.

Other than that, PVDF membranes had been extensively employed as the inorganic membrane due to its outstanding properties such as high stability of temperature, good mechanical strength and able to resist wide range of chemical substances (Subasi & Cicek, 2017). PVDF was a specialised plastic that is made using a variety of polymerization processes. Solvents were the primary auxiliary material utilised in the creation of PVDF membranes, and they were used in a variety of membrane fabrication techniques to dissolve the PVDF. PVDF membrane had hydrophobic nature which is identical to the PES membrane. When the PVDF membrane was used in water, the undesired particles and matter contained in water were prone to forming deposits on the membrane's surface. This leads to the decrease in water permeability as well as generate fouling occurrence. Therefore, the modification of PVDF membrane’s surface with the additional of other material was considered to improve the hydrophilicity of the membrane.

Last but not least, PSf was one of the most prominent polymers used in membrane fabrication due to its commercial availability and ease of processing. Moreover, Tan &

Rodrigue highlighted that PSf provides had a high thermal resistance, chemical tolerance to wide range of pH and excellent mechanical strength properties (Tan & Rodrigue, 2019). Generally, PSf membrane was synthesized via phase inversion method for water treatment application. It was extensively applied in the water purification mechanism such as MF and UF mechanisms. PSf membranes had also been developed for water separation operations to eliminate suspended particles, colloids, proteins, oils, metal hydroxides, bacteria, pyrogens, and other contaminants from water and wastewater (Kheirieh *et al*., 2018). Membrane fouling and wetting were two key issues associated with the use of PSf membranes, both of which shorten the membrane's lifespan. In summary, hydrophilic alteration was used to improve the antifouling and anti-compaction properties of PSf membranes.

In a nutshell, PSf membrane was employed in this research to study due to its beneficial properties. The introduction of the second material phase was suggested as a way to overcome the membrane fouling as well as to improve the overall performance of PSf membrane. Various inorganic membranes had been incorporated into polymeric materials so that the mechanical and physico-chemical properties of the polymer membrane was enhanced. The study of various types of inorganic membranes were presented in the following section.

2.3.2 Inorganic membrane

The most common inorganic membranes were metallic, ceramic, and zeolite membranes, as stated by Asad *et al.* (Asad *et al.*, 2020). Inorganic membranes, such as metals or ceramics, have superior mechanical, chemical, and thermal qualities to polymeric membranes, but they were more expensive to manufacture and hence were not chosen (Asad *et al.*, 2020). Even though inorganic membranes were more expensive than polymeric membranes, they offer benefits such as the ability to withstand harsh chemicals and frequent backwashing, the ability to be sterilized and autoclaved, high temperature and wear resistance, a well-defined and stable pore structure, high chemical stability, and a long life span. Their biggest disadvantages, however, were their high cost and stiffness (Kavyani *et al.*, 2018). There were several types of inorganic membranes including ceramic membrane, silica membrane, zeolite membrane and clay mineral-based membrane.

One of the common inorganic membranes was ceramic membrane. Ceramic membranes were typically comprised of titania, silica, alumina, and zirconia, and were made up of more than one layer of raw materials, generating an asymmetric structure (Rani & Kumar, 2021). According to Kavyani *et al.*, a macro-porous support, a meso-porous intermediate layer, and a top layer were the three porosity layers that make up a ceramic membrane's asymmetrical structure (Kavyani *et al.*, 2018). The membrane's mechanical strength was provided by the macro-porous support, which minimizes mass transfer resistance, while the membrane's selectivity and separation efficiency were provided by the top layer. As compared to polymeric membrane, ceramic membrane has better temperature and chemical stability, corrosive resistance, cleaning ease, and a longer lifespan (Rani & Kumar, 2021). Additionally, due to their durability and chemical stability, as well as their ability to eradicate microbes, organic material, and disinfection wastes, ceramic membranes were one of the viable options in wastewater treatment systems when the condition is hostile. One of the benefits of using ceramic membranes was that their hydrophilic properties make them less susceptible to organic fouling than polymeric membranes. In comparison to a smoother and smaller pore size membrane, the ceramic membrane with the roughest surface and largest pore size had the highest risk for fouling, as stated by Kavyani *et al.* (Kavyani *et al*., 2018). High quantities of organic matter and bacteria in water, on the other hand, can produce membrane fouling, which reduced flux (Kavyani *et al.*, 2018). Besides, Rani and Kumar stated that the high cost of raw materials and greater sintering temperatures were limiting considerations for the commercialization of ceramic membranes (Rani and Kumar, 2021).

Next, silica membranes were commonly employed in industrial applications at high temperatures and simultaneous reactions and separation processes, as stated by Liu *et al.* (Liu *et al.*, 2017). It had a high retention capacity of water and able to retain water under high temperature state, thus silica membrane had the potential to be one of the most attractive filler in membrane technology (Ying *et al.*, 2018). The great selectivity, thermal resistance, cost-effective and chemical resistance of silica membranes were widely recognized. Besides, long-term operating stability was another advantage of using silica membranes. Moreover, the mechanical strength of a membrane was influenced by its silica content, with proper silica loading increasing the strength. However, one of the drawbacks of silica membranes was that they encounter hydro-instability issues and degrade structurally when exposed to water in which consequently losing their selectivity. This process happened as water molecules on the

silanol functional group rehydrate the silica surface through the physisorption process then followed by chemisorption with the siloxane functional group. Thus, the hydrolysis reaction occurs in which siloxanes operate as strong acid-base sites with a high absorption of water molecules, allows the siloxane group to split and allow dissociative chemisorption (Kavyani *et al.*, 2018). Apart from that, due to the difficulty of diffusing into the polymer framework and occupying the water swollen pores, large silica particle sizes that surpass the maximum swelled pore size of the polymer experienced a decrease in proton conductivity. Increased silica loading in the membrane resulted in a severe dilution effect for the membrane's ion exchangeable groups. This indicates that when the amount of uncharged or pure silica in the membrane grows, the ion exchange capacity of the membrane decreases. As mentioned earlier, the mechanical strength of silica membrane was enhanced with optimal content of silica. Excessive silica content, on the other hand, causes membrane homogeneity to be lost, causing the membrane to become brittle. Furthermore, due to the inherent tendency of silica particles to re-agglomerate, a high silica concentration will generate a higher rate of agglomeration in the membrane morphology (Ying *et al.*, 2018).

Zeolite membranes were inorganic membranes that are made up of a thin layer of polycrystalline zeolite film that grows on top of a substrate (Nazir *et al.*, 2020). The zeolite pores were made up of rings in the framework that are chosen based on the number of oxygen atoms that make up the ring, which can have a variety of structures and matrices. Most of the features, such as membrane wettability and membrane surface charge, were regulated by the ratio of silica and aluminium in the zeolite structure. Kavyani *et al.* reported that the surface hydrophilicity and water affinity of the membrane were controlled by the aluminium content of the zeolite structure (Kavyani *et al.*, 2018). Due to its strong qualities and high separation performance, zeolite membrane had received much interest and it can be a good candidate in water treatment industry especially when there were high content of organic. In addition, Nazir *et al.* revealed that due to their appealing characteristics such as adaptability to harsh environments, long-term stability at high temperatures and pressures, molecular sieving, catalytic, and selective sorption properties, zeolite membranes offer several advantages over organic membranes and other types of inorganic membranes (Nazir *et al.*, 2020). In contrast, zeolite membranes can be a competitive choice for various desalination procedures that require the removal of dissolved cations due to their cation exchange capabilities. Since zeolite membranes were often quite expensive, industrial applications of zeolite membranes for

desalination processes are limited. Furthermore, fabricating a defect-free zeolite membrane with a reasonable thickness was incredibly challenging (Kavyani *et al.*, 2018). Intercrystalline voids or nonzeolitic pores that were larger than zeolite pores are used to identify defects. Thus, the occurrence of faults in the membrane layer must be reduced because they will have a major impact on the membrane's quality and function (Nazir *et al.*, 2020).

Additionally, clay minerals were considered to be the ideal option as the inorganic membrane for removing a wide range of contaminants from the environment. This was because they provide high specific surface area, surface hydrophilicity, porosity, cation exchange capacity, chemical stability, varied expansibility, reactive functional groups, and surface charge as stated by Dutta *et al*. (Dutta *et al*., 2021). Clay minerals as inorganic membranes had the advantages of being naturally prevalent, nontoxic, easily mined, and generally inexpensive materials. The outer and inner surfaces of most clay minerals were hydrophilic and polar, resulting in strong affinities for low and high-molecular, mostly cationic, compounds (Perelomov *et al*., 2021). Clay minerals were a type of mineral that found near the planet's surface and formed due to the rock chemical weathering. Clay minerals were significant soil elements that occur when rocks undergo diagenetic and hydrothermal alteration in the presence of water. They were typically found in fine-grained sedimentary rocks and due to the existence of an imbalanced electrical charge on their surface, clay minerals have the ability to store water and dissolved plant nutrients eroded from other materials (Kumari & Mohan, 2021). Next, a critical review of layered clay minerals including kaolinite, chlorite and MMT were presented.

Kaolinite was a 1:1 clay mineral with chemical formula of $Si_4Al_4O_{10}(OH)_8$. It was made up of paired oxygen atoms and hydroxyl ions that have hydrogen bonding between them, resulting in triclinic symmetry with neutral electrostatic properties. In kaolinite, there was also a fundamental unit consisting of a silicate groups two-dimensional layer connected to a aluminate groups layer (Massaro *et al*., 2018). In lower kaolinite minerals crystallinity, common random movement between the layers were obtained due to weak hydrogen bonding. Additionally, there was no charge in ideal kaolinite structure, and the structure was stable due to the bonding of hydrogen molecules. As mentioned by Kumari & Mohan, kaolinite does not swell in water as the clay was wetted, thus there was no expansion between the layers (Kumari & Mohan, 2021). Kaolinite was also discovered to have a low surface area and cation exchange capacity, implying that the clay has less molecular interaction when used to treat heavy metals (Kumari & Mohan, 2021). One of the reasons regarding to low cation exchange capacity in

kaolinite was due to the infertility of soils, as reported by Massaro *et al.* (Massaro *et al*., 2018). Overall, kaolinite was favorable in terms of its inertness, welling properties, sorption capacity, and low surface area.

Apart from kaolinite, chlorite was also a type of clay mineral that mainly belongs to 2:1:1 silicate group with ideal formula of $Al_{4.3}(Si_3Al)O_{10}(OH)_8$ (Kumari & Mohan, 2021). It was mostly made up of iron magnesium silicates with a few aluminium atoms thrown in for good measure. The characteristic chlorite clay crystal was generally alternated with a brucite layer. Brucite layer refers to the magnesium-dominated tri-octahedral sheet in which magnesium ions occupied all the octahedral positions in chlorite. One of the peculiar qualities of chlorite was that there is no water adsorption between the layers, which accounts for the mineral's non-expanding nature (Kumari & Mohan, 2021). Eventually, chlorite was considered as low cost material due to no adsorption of water between the layers. Moreover, Bourdelle stated that chlorite had a broad thermal stability range, and its chemical composition was impacted by the system's chemistry, oxygen fugacity, and temperature and pressure circumstances (Bourdelle, 2021). Thus, a systematic variations in the chlorite chemical composition was attained wide range of temperature properties (Fulignati, 2020). Similar to kaolinite clay mineral, chlorite had low cation exchange capacity which became the main drawbacks in removing heavy metals in water, as mentioned by Nadziakiewicza *et al*. (Nadziakiewicza *et al*., 2019). This was because heavy metals considered as cation molecules, thus in removing them, a high cation exchange capacity was favorable. In short, chlorite can be applied when properties such as non-expanding nature, low cost, thermal stability, low cation exchange capacity was desired.

Besides, MMT was one of the clay minerals used as the inorganic membrane for the fabrication of MMM with PSf. Due to isomorphous replacement by cations in the octahedral layer, negative charges arise on the surface of MMT (Shokri *et al*., 2021). The presence of hydroxyl groups in MMT was beneficial for adsorption of heavy metals ions (Mahmoudian *et al*., 2018). MMT consists of inter-layer cations that were easily exchangeable by other cationic molecules via interaction of electrostatic or ion exchange, thus making it susceptible to remove heavy metals from water and wastewater (Abdel-Karim *et al*., 2021). In contrast, Mahmoudian *et al*. described that MMT had limitation in terms of dispersion (Mahmoudian *et al*., 2018). This was because MMT tends to agglomerate, causing membrane permeability and antifouling effectiveness to deteriorate. Therefore, the effect of MMT loading was investigated to

determine the optimum performance of MMM in removing heavy metal. To sum up, MMT was the viable option to fabricate into PSf to produce MMM and enhance the membrane filtration performance. The benefits include limit formation and proliferation of macrovoids, high number of small surface pores, boost surface hydrophilicity, high porosity and water permeability, enhanced mechanical characteristics, and improved antifouling property.

2.3.3 Mixed Matrix Membrane

Mixed matrix membrane (MMM) referred to membranes that consists of polymers filled with inorganic membranes or the addition of same type of membrane that able to improve the chemical and physical properties of the membrane. In this research study, PSf was used as the polymer membrane meanwhile MMT was utilized as the inorganic membrane to fabricate MMM. There were several literature works were reviewed and discussed in terms of organic membrane, inorganic membrane, membrane mechanism, water flux, heavy metal, and removal capacity. The literature works based on water filtration module were summarized in **Table 2.1**.

In the study of Jacob *et al*., an UF membrane was executed which comprised of PSf and MMT as the polymer and inorganic membrane respectively with addition of polyvinylpyrrolidone (PVP) as porogen (Jacob *et al*., 2020). The usage of PVP contributes to the increment of the membrane porosity and water uptake. It was found that the MMM has higher heavy metal rejection and better antifouling property as compared to the pristine membrane. Despite of the advantages, the MMM also had several limitations. One of them was PVP is known to be non-biodegradability, as stated by Kurakula & Rao (Kurakula & Rao, 2020). Besides, the effectiveness of membrane surface area was reduced when the concentration of MMT was above 3wt% due to agglomeration (Jacob *et al*., 2020).

Aside from that, Abd Hamid *et al*. developed a MF membrane which consists of polymeric membrane and inorganic membrane made of PSf and zeolite respectively (Abd Hamid *et al*., 2021). Sodium dodecyl sulfate (SDS) and PVP were used as the additives to improve the pore size of the MMM. The MMM has several advantages including high hydrophilicity, high rejection percentage of copper ions in water, high degree of flexibility and low cost. Nevertheless, the study of PSf/zeolite membrane did not consider the fouling phenomenon. The analysis of fouling phenomenon was crucial to evaluate the mechanism of

membrane's blocking during filtration. Besides, the filtration flux was reduced as the amount of inorganic membrane increased. This might be due to the zeolite particles that deposit on the membrane causing pore blockage and lower permeability (Abd Hamid *et al*., 2021).

Apart from that, MMM of PSf and $NiFe_2O_4$ nanoparticles were fabricated with N, N-dimethylformaamide (DMF) as the additive as studied by Mondal *et al*. (Mondal *et al*., 2017) in terms of characterization of nanoparticles and fabricated MMM, permeability, contact angle, heavy metal removal capacity, and permeate flux. There were several heavy metals are selected in the literature including copper, cadmium, nickel, zinc, lead, and chromium. It was observed that this MMM had high permeability, hydrophilic characteristic, high removal of heavy metals, and high permeate flux. Furthermore, the increase of nanoparticles concentration in the polymer membrane was evaluated in which high concentration of nanoparticles provides better performance of MMM. Membrane fouling analysis was not considered in this study of which become the limitation of the authors' study.

Other than that, Delavar *et al*. fabricated polycarbonate (PC) and hydrous manganese oxide (HMO) to produce UF membrane (Delavar *et al*., 2017). The analysis including characterization of MMM as well as the evaluation of pure water flux, mean pore size, porosity, contact angle, and cadmium and copper ions removal via different loading of HMO were considered in this study. Overall, the fabricated MMM offerred several benefits to treat heavy metals such as low cost material and low pressure requirement are obtained. Nonetheless, the agglomeration of HMO may occurs resulting in the reduction of HMO contact area. This can be prevented by conducting a proper procedure of casting solution preparation so that a better distribution of HMO was attained.

According to the literature of Chandrashekhar *et al*., mixed matrix ultrafiltration membrane is fabricated that comprised of polyphenysulfone (PPSU) and multiwalled carbon nanotubes ($MWCNT_s$) (Chandrashekhar *et al*., 2019). The characterization of the fabricated membrane were analysed which includes the contact angle, porosity and water uptake, membrane morphology, pure water flux, antifouling property, and rejection analysis of lead, mercury and cadmium ions. Based on the result and discussion of the study, high membrane porosity, high pure water flux, improved antifouling property, high removal efficiency of heavy metals were achieved. In contrast, it was found that higher concentration of $MWCNT_s$ contributes to low hydrophilicity due to impulsive movement of $MWCNT_s$ to membrane/liquid

partition resulting in lower interfacial energy. In short, the concentration of inorganic membrane contributes to the performance of the MMM.

Last but not least, cellulose acetate (CA) was employed with the addition of poly (methyl vinyl ether-alt-maleic acid) (PMVEMA) as additive to fabricate MMM, as studied by Lavanya *et al*. (Lavanya *et al*., 2019). The fabricated membrane was considered as the UF membrane which had several advantages including increased surface hydrophilicity, increased porosity, high thermal stability, increased pure water flux, high porosity, enhanced antifouling property, and effective in removing lead, cadmium and chromium ions in water. Contrarily, it was determined that the fouling resistance was enhanced if the concentration of PMVEMA was considered as one of the limitations in this study. This was because high material cost is introduced due to high requirement of additive in the MMM. To sum up, CA-PMVEMA membrane had a good potential in treating heavy metal due to its enhanced hydrophilicity, permeability and antifouling property when high concentration of PMVEMA is considered.

In conclusion, there was limited study that analyse the physical and chemical properties of the PSf/MMT membrane. Therefore, a critical study to remove heavy metals such as cadmium and lead was conducted by using PSf/MMT membrane.

Table 2.1: Literature review of MMM for heavy metal removal

Organic membrane	**Inorganic membrane/ Additives**	**Membrane mechanism**	**Water flux**	**Heavy metal** ***Feed concentration***	**Removal capacity**	**Citation**
PSf	MMT/PVP	UF	102 $L/m^2.h$	Cr **Feed concentration = 5 ppm*	89%	Jacob *et al.* (2020)
PSf	Zeolite	MF	25 $L/m^2.h$	Cu **Feed concentration = 10 mg/L*	96.4%	Abd Hamid *et al.* (2021)
PSf	$NiFe_2O_4$	UF	30 $L/m^2.h$	Cu Cd Ni	98.6% 71.38% 62.51%	Mondal *et al.* (2017)

				Zn Pb Cr ** Feed concentration = 50 mg/L*	83.45% 98.14% 52.84%	
PC	HMO	UF	506 $L/m^2.h$	Cd Cu ** Feed concentration = 40 mg/L*	98%	Delavar *et al.* (2017)
PPSU	$MNCNT_s$	UF	185 $L/m^2.h$	Pb Hg Cd ** Feed concentration = 50 ppm*	98% 76% 72%	Chandrashekar *et al.* (2019)
CA	PMVEMA	UF	50 $L/m^2.h$	Pb Cd Cr ** Feed concentration = 10 ppm*	85.42% 72.21% 26.72%	Lavanya *et al.* (2019)

2.4 Fabrication of membrane

There were several methods for the fabrication of membrane such as electrospinning, stretching, track etching, and phase inversion. A comprehensive knowledge of each fabrication methods were included in terms of their benefits and drawbacks application.

Electrospinning was an electrostatic fibre-formation process that uses a range of polymers to create highly porous nanofibrous membranes. Interconnected open holes structure, high porosity, pore diameters ranging from several micrometers to tens of nanometers, and high surface-area-to-volume ratio were several advantages of electrospun nanofibrous

membranes. The uniaxial stretching of a viscoelastic solution governs the creation mechanism of electrospun fibres. In a normal electrospinning setup, a polymer solution was charged from a spinneret needle to a collector by supplying a high voltage difference large enough to increase the repulsive force within the charged solution to overcome its surface tension, producing a jet to erupt from the spinneret tip. In order to produce diverse electrospun nanofibrous membrane morphologies, the electrospinning settings and polymer solution characteristics can be altered (Asad *et al.*, 2020). Based on the study of Liao *et al.*, the authors discussed the advantages and disadvantages of electrospinning in fabricating MMM (Liao *et al.*, 2018). High level of versatility allows control over nanofiber diameter, microstructure, and arrangement, vast material selection, easy to incorporate additives in nanofibers, high porosity above 90% and high surface-to-volume ratio, one-step and straightforward process, and practicability in generating nanostructures were all advantages of fabricating MMM via electrospinning. In contrast, electrospinning makes it difficult to create nanofibers with diameters less than 100 nanometers and electrospun nanofiber membranes with maximum pore sizes less than 100 nanometers. Finally, the yield speed of electrospinning was slow (Liao *et al.*, 2018).

Besides, stretching was widely employed to fabricate MF and UF membranes. This was a solvent-free approach that involves heating a polymer past its melting point, extruding it into a thin film, then stretching it to create a porous structure. Stretched membranes were usually prepared in two steps which are cold stretching followed by hot stretching. Cold stretching creates micropores in the film, whereas hot stretching regulates the membrane's structure. For highly crystalline polymers, stretching was preferred because the crystalline areas provide strength while the amorphous regions provide flexibility to build porous structures (Asad *et al.*, 2020). According to Liao *et al.*, stretching method can prepared symmetric membranes with mean pore sizes between 0.1 and 3 microns, had ladder like slits, have porosity between 60% to 80% and can be used chemically stable materials such as polytetrafluoroethylene (PTFE), polyethylene (PE), polypropylene (PP) and ceramics (Liao *et al.*, 2018). Nonetheless, stretching requires high temperature to operate (Liao *et al.*, 2018).

Other than that, track etching was also used in fabricating membrane. In track etching, there were two steps are involved to fabricate membrane. A polymeric film was bombarded with energetic heavy ions in the first phase, damaging the chemical bonds in the polymer and generating linear tracks across the film. Then, in the second phase, the chemical etching technique involved chemically etching the damaged tracks to create empty channels. Track-

etched membranes allow for precise pore size distribution adjustment. Furthermore, pore density and pore size were independent factors that can be varied widely, allowing for a more straightforward relationship between water transport capabilities and membrane shape. Due to the great mechanical strength and resilience against acids and organic solvents, polyethylenenaphthalate (PET), polypropylene (PP), and polycarbonate (PC) were the most widely utilized materials for track-etched membranes (Asad *et al.*, 2020). The primary features of track etching were that it may produce symmetric membranes with mean hole sizes ranging from 0.02 to 10 microns, as well as narrow pore sizes distribution and cylindrical pores. Nevertheless, the disadvantages of track etching include a lack of appropriate polymers, a low porosity of 10%, and a high cost (Liao *et al.*, 2018).

Last but not least, the most versatile method for preparing membranes was phase inversion, which allows for a variety of morphologies to be obtained for various applications. The precipitation of a polymer from an initially homogenous casting solution was the basis for all phase inversion membranes. The precipitation occurs as a result of a demixing process in which a polymer solution was changed from a liquid to a porous solid state as a result of a solvent-nonsolvent exchange. The thermodynamics and kinetics of the phase inversion process control the precipitation of polymer solution, which had an impact on the final shape of produced membranes. The formulation of the casting solution, that was, the type and concentration of polymer, solvent, and additives, can be changed to influence thermodynamic and kinetic parameters (Asad *et al.*, 2020). The advantages of using the phase inversion method include the ability to use a wide range of polymers, the ability to fabricate fat-sheet and tubular membranes, ease of preparation and scaling up, fast yield speed, easy to optimize membrane thickness and pore size, high porosity of around 80%, and the ability to naturally form small surface pores and large bulk pores. Finally, the polymer must be soluble in a solvent or solvent mixtures in order to perform the phase inversion approach. In conclusion, phase inversion technique exhibited a number of benefits as compared to the other methods for fabricating MMM. The benefits were in terms of wide usage of polymers, simplicity, speed, optimum membrane thickness and pore size, high porosity, and natural formation of small surface pores and large bulk pores.

2.5 Summary

In a nutshell, extensive research on heavy metal removal was necessary, including the negative impacts to public health, permissible limit, and particle size, in order for the membrane separation process to function completely and properly. This chapter also covered the fundamentals of membrane filtering mechanisms. The in-depth understanding of most common used organic membranes and inorganic membranes were provided. Moreover, the evaluation of various types of layer silicates clay minerals were discussed thoroughly. The literature on MMM fabrication was evaluated in terms of the types of organic and inorganic membranes, membrane mechanisms, water flux, types of heavy metals and their concentrations, removal capability, as well as the membrane's pros and cons. Apart from that, the advantages and disadvantages of the different membrane fabrication methods were reviewed. Finally, the MMM comprised of PSf and MMT was fabricated by using phase inversion technique to remove copper and lead.

CHAPTER 3

METHODOLOGY

3.1 Methodology Framework

In this chapter, the procedures and techniques used to conduct this research were outlined. An experimental flowchart was developed as presented in **Figure 3.1** which employed as the guideline for this research.

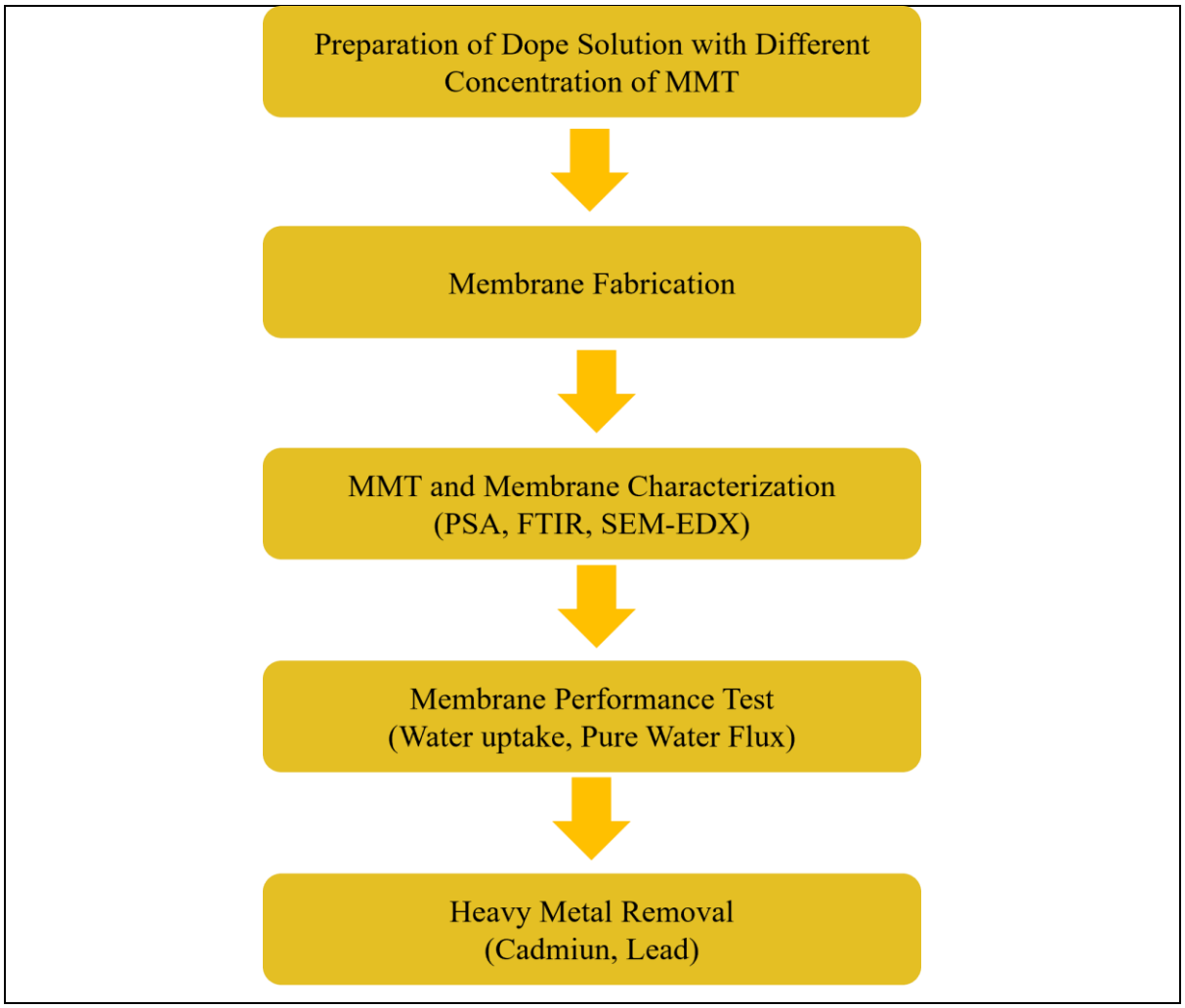

Figure 3.1: Experimental flowchart

Initially, the dope solution with different concentration of MMT was prepared followed by membrane fabrication via phase inversion technique. There were three different concentrations of MMT employed to fabricate with MMM including 0.5% (0.5MMM), 1.0% (1.0MMM) and 1.5% (1.5MMM). Next, the MMT and membrane characterization were conducted using PSA, FTIR and SEM-EDX analysis. PSA was used to analyze the particle size distribution of MMT whereas FTIR was employed to determine the functional groups for both MMT and the prepared membrane. As for SEM-EDX, the analysis was carried out to observe the membrane morphology including membrane cross section, membrane top surface and membrane bottom surface. Lastly, the performance of prepared membranes were evaluated in terms of water uptake, pure water flux and heavy metal rejection. Water uptake analysis to know the membrane capability to absorb water. The permeability of the membrane was evaluated by using pure water flux analysis and the prepared membrane were tested to remove cadmium and lead in water.

3.2 Materials

There were several materials are necessary to fabricate MMM including PSf in clear pellet form was obtained from Sigma Aldrich, Alkyl Quaternary Ammonium Bentonite also referred as MMT in powder form was acquired from BYK, N-methyl-2-pyrrolidone solvent (NMP, 99%, Sigma Aldrich), and distilled water.

3.3 Fabrication of MMM

The fabrication of MMM involved the preparation of dope solution and membrane. The detailed procedures in fabricating MMM were explained in the following section.

3.3.1 Dope preparation

As illustrated in **Table 3.1**, four distinct membranes were fabricated utilising PSf dope solutions, namely pristine PSf membrane, 0.5MMM, 1.0MMM and 1.5MMM. For pristine PSf preparation, the weight of NMP solvent was measured in a 100 mL Schott bottle containing a magnetic stirrer bar until reached 85g. Next, the weight of PSf pellet was measured until reached 15g. The Schott bottle was placed onto a magnetic plate stirrer, then the PSf pellet was added into the NMP solvent gradually. The mixture was stirred continuously for 24 hours to obtain homogeneous state. As for dope solution containing MMT, notably 0.5MMM, 1.0MMM, and 1.5MMM, an appropriate amount of MMT was added into the NMP solvent and let the mixture mixed about one minute on the magnetic plate stirrer. Let the MMT dried in the oven overnight at 60℃ in a beaker before being mixed with NMP solvent. Following that, the mixture was sonicated for 30 minutes at ambient temperature. Identical to the preparation of pristine PSf membrane, the PSf pellet was added gradually into the mixture after sonication process. The stirring process took about 24 h at ambient temperature.

Table 3.1: The composition of dope solution for MMM

Membrane	**Dope solution composition**		
	PSf (wt%)	**MMT (wt%)**	**NMP (wt%)**
Pristine PSf	15	0.0	85.0
0.5MMM	15	0.5	84.5
1.0MMM	15	1.0	84.0
1.5MMM	15	1.5	83.5

3.3.2 Membrane Preparation

A cleaned glass plate and metal rod were prepared for membrane casting process in which the glass plate was taped both sides to avoid the spillage of dope solution. Next, an appropriate amount of dope solution was poured on top of the glass plate. The dope solution is then casted by using metal rod. After casting, the coated glass plate was immersed in a water coagulation bath at room temperature until the membrane detached from the glass surface.

Subsequently, the casted membrane is transferred to another water bath and further immersed for at least 24 h to remove residual. Lastly, it was kept in distilled water till next use.

3.4 Montmorillonite (MMT) Characterization

3.4.1 Particle size analyzer (PSA) Analysis

Particle size analyzer (PSA) analysis, also known as laser diffraction technique, was a well-known method for measuring a sample's particle size distribution by examining the scatter pattern of light from the sample. In this study, CILAS 1090 Liquid model (**Figure 3.2**) was employed to evaluate the particle size distribution of MMT. A laser beam was directed onto dispersed particles, then the laser light was diffracted by the particles. An array of sensors detects and evaluates the corresponding diffraction pattern. It was possible to quantitatively derive particle size information from the scattered light of an observed sample since the angle and intensity of the scatter pattern was a function of particle size. The diameter of the sphere of equivalent volume of the observed particle was used to generate a volume fraction distribution for particle size information for a particular sample. The steps required to perform PSA analysis were presented by referring to the study of Centeri *et al*. (Centeri *et al*., 2015). Initially, an appropriate amount of MMT was measured in a diffractometer. Permanent ultrasonic disaggregation was used throughout several minutes measuring period. Finally. a Fourier lens collected the diffracted rays onto the detector. The calculation method was based on the Mie theory, which uses the intensity of the diffracted light pattern to forecast particle size distribution.

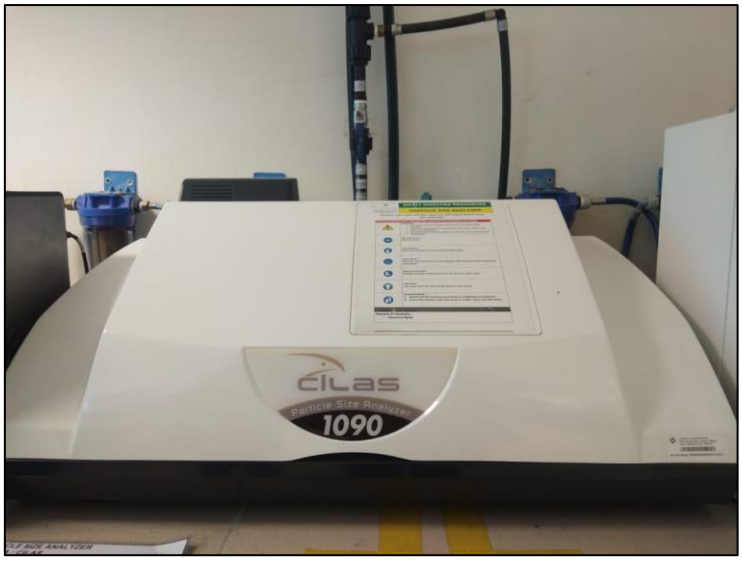

Figure 3.2: Particle Size Analyzer (PSA) equipment

3.4.2 Fourier Transform Infrared (FTIR) Analysis

Fourier transform infrared (FTIR) spectroscopy was one of the most powerful tools for the determination of functional group in a material together with possible molecular bonds between chemical compounds of material. The FTIR model used in this study was Shimadzu IRAffinity-1 as shown in **Figure 3.3**. The FTIR analysis was conducted via the preparation of blank potassium bromide (KBr) and MMT sample. To begin, the capsule press equipment as well as mortar and pestle were carefully cleaned with chloroform and then dried using tissue. Some dried KBr were scooped out into the mortar and grinded well with MMT powder using the pestle to obtain homogeneous mix. Then, the pellet press was fixed together by putting the upper body and gently turned it into the lower body. A dyne was inserted into the cavity and make sure it sits on top of the basement. Next, the grinded KBr was transferred into the cavity using a metal spatula. The bolt press was inserted and rotated into the cavity to distribute the particles. The second dyne was then inserted and the bolt press was adjusted onto it. The whole entity was transferred into the hydraulic press and the wheel was turned to secure it then the knob was rotated clockwise to tighten it. Subsequently, the lever was pulled repeatedly and wait for about two minutes for it to be compressed. In order to release pressure, the knob was rotated counter clockwise. After that, the wheel was turned to disengage the pellet press and disassemble the press entity. The upper body was inverted and placed on top of the lower body.

The adapter was assembled on top of the upper body and the wheel was rotated slowly until the dynes were loosened. The force was applied at the middle of the press and make sure that the giant screw was a top of the press entity in which there were no gaps between the screw, the adapter and the press entity. The entity was removed from the hydraulic press then the upper dyne was lifted up in which a nice blank KBr disc was formed. Then, the KBr disc was transferred into the sample holder and cap was fixed on the sample holder. The sample holder was placed into the FTIR machine. Lastly, a sample scan was performed and the results were obtained.

Figure 3.3: Fourier Transform Infrared (FTIR) equipment

3.4.3 MMT powder morphology

Scanning Electron Microscopy-Energy Dispersive X-Ray (SEM-EDX) analysis entailed scanning the MMT's surface with an electron focussed beam to determine the morphology of the particle. Chemical composition and elemental investigation were investigated using a combination of SEM and EDX analysis, resulting in a detailed metallurgical evaluation. Each element produces X-rays of certain energies and wavelengths characteristic of the element very instantly as it returns to its original energy state. With the X-ray wavelength on the x-axis and intensity on the y-axis, EDX spectroscopy showed these data and identified each appropriate element. The elements were identified by comparing the peak values on the x-axis to known wavelengths for each element in order to determine the sample's

elemental composition. Based on **Figure 3.4**, the SEM-EDX equipment was using the model of Hitachi TM4000 Plus. This can be done by obtaining a suitable amount of MMT sample which was lightly sprinkled on the carbon tapes and pushed into place with a spatula. To remove loose material, the sample holder was turned upside down and tapped. Finally, the sample holder was loaded into SEM chamber for further analysis.

Figure 3.4: Scanning Electron Microscopy (SEM) equipment

3.5 Membrane Characterization

3.5.1 Fourier Transform Infrared (FTIR) Analysis

The pristine PSf and MMM were analysed by using FTIR analysis. The membrane sample were directly placed at the tip of the FTIR chamber for scanning. After placing the sample in the spectrometer, the collection of spectra was started and the lid of the chamber should be closed. Consecutive transmission spectra was recorded by collecting any number of scans per spectrum. Finally, the sample was removed from the machine after the scanning process.

3.5.2 Membrane morphology

SEM combined with EDX was used to examine the morphology of the prepared membranes, implying that the prepared membrane samples for SEM can be studied directly by EDX. The procedures to conduct SEM-EDX analysis for membrane was obtained from the literature of Alqaheem & Alomair (Alqaheem & Alomair, 2020). Initially, the prepared membrane samples were cut into smaller pieces to fit on the specimen stage. It was advisable to immerse the membrane samples in liquid nitrogen for several minutes to obtain a better image and eliminates surface bend. Then, cut it by a sharp blade or let it fracture spontaneously. Next, the samples were coated with a conductive material, particularly gold in this study. This action was required due to the weak conductivity in most polymers and to improve the quality of the analyzed images. This was because coating decreases the thermal damage caused by charge build-up on the membrane sample. Since the coating material may be detected in the EDX spectrum, it was important to select an appropriate coating material to avoid overlapping with the elements present in the produced membrane sample.

3.5.3 Water uptake

Initially, a small circular prepared membrane with diameter of 2 cm was utilized for water uptake analysis. The dry weight of each membrane was measured by using analytical balance. Next, the similar membrane was immersed in distilled water up to 24 h. Following that, the excess water from the membrane surface was removed and the weight of the wet membrane was measured. Finally, the water uptake results were assessed by using **Equation 1** (Jacob *et al*., 2020).

$$\text{Water uptake (\%)} = \left(\frac{W_w - W_d}{W_w}\right) \times 100\% \qquad \textbf{Equation 1}$$

where,

W_w = Membrane wet weight

W_d = Membrane dry weight

3.6 Membrane Performance

3.6.1 Pure Water Flux

First and foremost, the prepared membrane was cut into a circular size with diameter of 6 cm. The fabricated membrane was fully immersed in distilled water for several hours, and the pure water flux was conducted by using water separation system (**Figure 3.5**) with constant pressure which was at 1 bar. The pure water flux and surface porosity were calculated using **Equation 2** and **Equation 3** respectively (Jacob *et al*., 2020).

Figure 3.5: Water separation system

$$J = \frac{Q}{A\Delta t}$$ **Equation 2**

where,

J = pure water flux (L/m^2.h)

Q = volume of collected permeate (L)

A = effective membrane area (m^2)

t = sampling time (h)

$$P = \frac{W_{wet} - W_{dry}}{\rho A h} * 100$$ **Equation 3**

where,

P = surface porosity (%)

W_{wet} = membrane weight at wet condition (g)

W_{dry} = membrane weight at dry condition (g)

ρ = density of water (1×10^6 g/m^3)

h = membrane thickness (m)

3.6.2 Heavy Metal Rejection

Standard solution of cadmium nitrate solution (0.0 ppm, 0.05 ppm, 0.10 ppm, 0.20 ppm and 0.50 ppm) and lead nitrate solution (0.0 ppm, 0.5 ppm, 1.0 ppm, 2.0 ppm and 5.0 ppm) were prepared from 1000 ppm by using dilution method. The standard solution for both heavy metals were examined by Atomic Absorption Spectroscopy (AAS), AA-7000 model (**Figure 3.6**) to obtain the calibration curve. Following that, the heavy metal rejection was conducted by using water separation system by employing the highest standard solution of heavy metals as the feed concentration. For instance, the feed concentration of cadmium nitrate solution was 0.50 ppm meanwhile lead nitrate solution was 5.0 ppm. The experiment was carried out at 1 bar and ambient temperature. Permeate was collected after obtaining steady state for 15 minutes and its volume was noted. The concentration of permeate as well as the standard solution of heavy metals were determined by AAS. Finally, the percentage rejection of heavy metal were calculated by using **Equation 4** as stated by Jacob *et al*. (2020).

$$\text{Percentage rejection of heavy metal (\%)} = \left(\frac{C_i - C_f}{C_i}\right) \times 100\% \qquad \textbf{Equation 4}$$

where,

C_i = Initial concentration of heavy metal (mg/L)

C_f = Final concentration of heavy metal (mg/L)

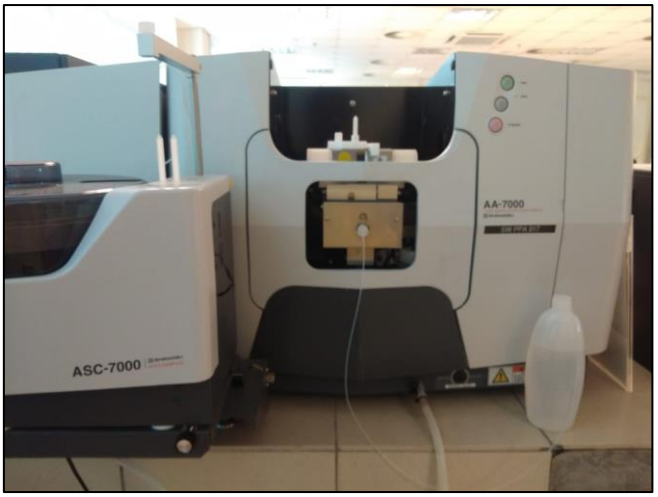

Figure 3.6: Atomic Absorption Spectroscopy (AAS) equipment

3.7 Summary

To summarise, the fabrication of MMM was accomplished utilising the phase inversion technique. Following that, chemical and physical properties of the MMT and prepared membrane were determined. The chemical properties of MMT and the prepared membrane were investigated using FTIR. On the other hand, the physical properties of MMT was evaluated by using PSA and SEM-EDX meanwhile the physical properties of the prepared membrane was studied by using SEM-EDX. Lastly, the performance of prepared membranes were carried out in terms of water uptake, pure water flux and heavy metal rejection. Water uptake analysis to know the membrane capability to absorb water. The permeability of the membrane was evaluated by using pure water flux analysis and the prepared membrane were tested to remove cadmium and lead in water.

CHAPTER 4

RESULT & DISCUSSION

4.0 Overview

In this chapter, the characterization of MMT powder were conducted via PSA, FTIR, and SEM-EDX analysis. Apart from that, the FTIR and SEM-EDX analysis were employed to evaluate the membrane characterization. The SEM-EDX analysis was conducted at three different spot on the membrane which were cross section, top surface and bottom surface. Then, the prepared membrane were characterized in terms of its water uptake to evaluate the membrane capability to absorb water. Finally, the membrane performance was executed in terms of pure water flux and heavy metal rejection.

4.1 Montmorillonite (MMT) Characterization

4.1.1 Particle size analyzer (PSA) Analysis

The Particle Size Analyzer (PSA) Analysis was carried out to evaluate the particle size distribution of MMT. The cumulative frequency of MMT mass fraction as well as density distribution of MMT were examined at wide range of MMT diameter. The particle size distribution of MMT was shown in **Figure 4.1** that presents the cumulative value and density distribution as a function of particle size diameter and the numerical value was provided in **Appendix**. It was observed that diameter at 10%, 50% and 90% of mass fraction were 3.74μm, 12.08μm and 24.30μm respectively. Thus, the mean diameter of MMT was 13.21μm. As illustrated in the figure, the sizes of most of the MMT particles lie within a wide range of 1.60μm to 45.0μm. The particle distribution was monomodal, with a peak at 16.0μm. Based on the work of Sankaranarayanan *et al*., the authors stated that the range of most MMT particles were within 5 - 50μm which indicates particles homogeneity and uniform particle size distribution (Sankaranarayanan *et al*., 2019) Besides, the clay powder was characterized with a laser particle sizer operated in the range of 0.08–2000μm which yields no particles with a size above 100 μm (Czarnecka-Komorowska *et al*., 2020). As shown in **Figure 4.1**, the distribution depicted that there was no particle size of clay powder greater than 100μm. Other

than that, Barakan & Aghazadeh studied that the particle size range by 10%, 50% and 90% of clay mass fraction which equals to 2.47, 11.18 and 24.20μm respectively with particle size mode of 14.52μm (Barakan & Aghazadeh, 2019). On the other hand, the clay particle size mode of the current study was obtained at 16.0μm which was the highest peak of density distribution. It can be observed that the data obtained by the authors had approximate values with the current data of particle size distribution. In summary, the particle size of clay used in this study had satisfactory agreement, as the particle size range, the value particle size for each mass fraction, and the particle size mode were all within the range of existing literature.

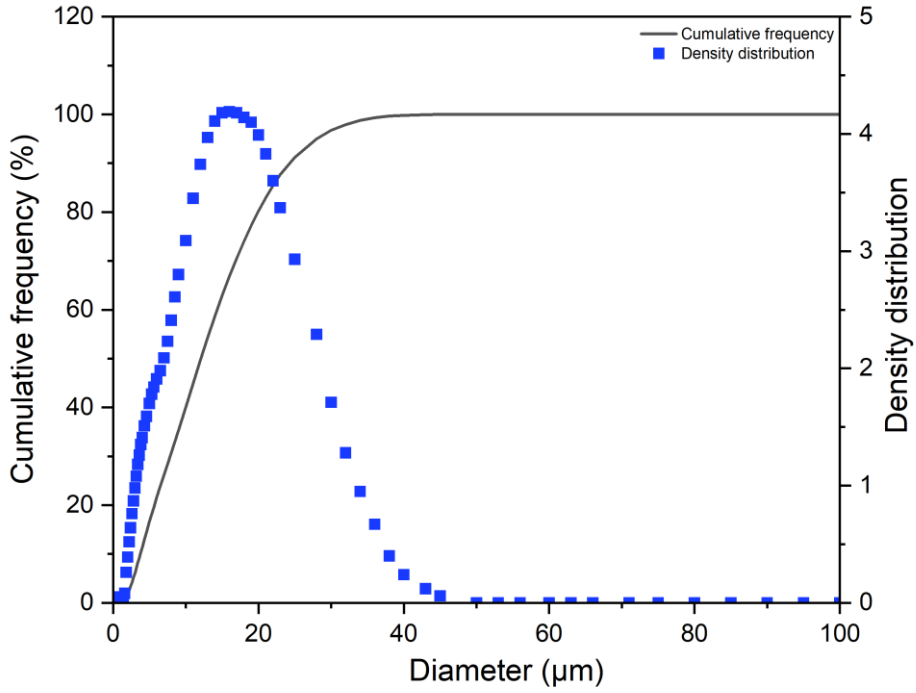

Figure 4.1: Particle size distribution of MMT powder

4.1.2 Fourier Transform Infrared (FTIR) Analysis

The FTIR analysis was conducted to determine the functional groups of MMT by considering the wavelength from 4000 – 400 cm^{-1}. Based on **Figure 4.2**, there are several significant peaks were obtained from MMT which located at wavelength of 3626 cm^{-1}, 1639 cm^{-1}, 1031 cm^{-1}, 918 cm^{-1} and 546 cm^{-1}. According to Caccamo *et al*., peak at 3626 cm^{-1} and 1639 cm^{-1} were attributed to O-H stretching and O-H bending (hydration) respectively (Caccamo *et al*., 2020) Band located at 3626 cm^{-1} was attributed to the O-H groups substituted

with the octahedral cations either aluminium, iron or magnesium cations (Caccamo *et al*., 2020). Other than that, wavelength at 1031 cm^{-1} represents Si-O stretching (Ashiq *et al*., 2019). Last but not least, Castellini *et al*. reported that peak at 918 cm^{-1} and 546 cm^{-1} were denoted as Al-OH-Al deformation and Al-O-Si deformation respectively (Castellini *et al*., 2017). This suggested that the presence of oxygen, silica and aluminium bonds play a vital role in obtaining MMT. Moreover, it was observed that there were several bands within the range of 3000 – 2750 cm^{-1}, indicating that impurities were presented in the specimen. To conclude, the crucial bands required for the MMT identification includes O-H stretching, O-H bending, Si-O stretching, Al-OH-Al deformation and Al-O-Si deformation.

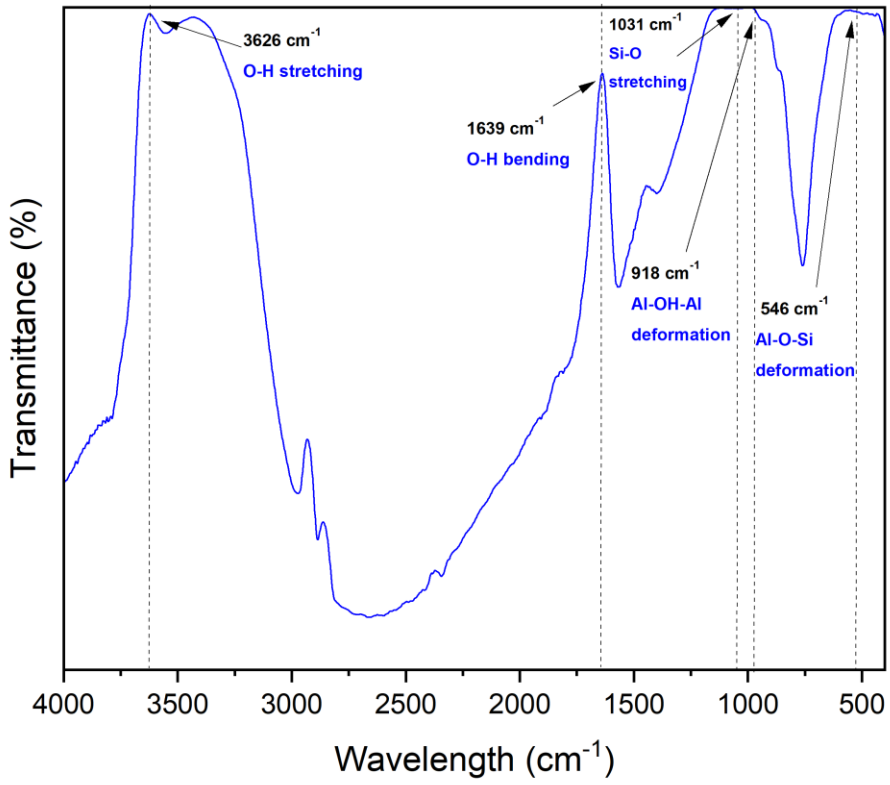

Figure 4.2: FTIR spectra of MMT powder

4.1.3 MMT powder morphology

The overall morphologies of the montmorillonite clay were examined by using SEM-EDX analysis at three different magnification including 500, 1000 and 5000 magnification. As illustrated in **Figure 4.3**, the MMT exhibits an irregular particle structure and was lumped

together as proven by Yaseen *et al*. (Yaseen *et al*., 2021). Besides, Ouardi *et al*. mentioned that the MMT clay's morphology could result in a high surface area and increased active sites, allowing for more effective mixing and a homogeneous dope solution (Ouardi *et al*., 2019). The MMT samples also formed agglomeration as the particles had a polydisperse pattern (Alekseeva *et al*., 2019). Therefore, MMT particles had several significant characteristics including irregular shape and polydisperse pattern that agglomerates, yielding effective mixing and a homogeneous dope solution due to their enhanced surface area and active sites.

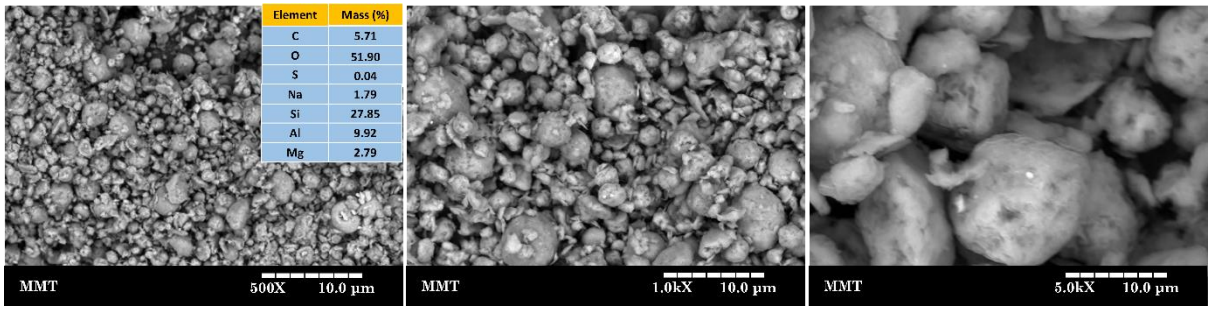

Figure 4.3: SEM images of MMT powder

As for EDX analysis, the elemental composition of MMT which was carried out at 1000 magnification. The EDX spectrum revealed that MMT clay mainly consist of carbon (5.71 wt. %), oxygen (51.90 wt. %), sulphur (0.04 wt. %), sodium (1.79 wt. %), silica (27.85 wt. %), aluminium (9.92 wt. %) and magnesium (2.79 wt. %) elements as provided in **Appendix**. The elements were proven by the studies of Mahmoudian *et al*. in which the most dominant peaks for MMT were belongs to oxygen, silica and aluminium atoms (Mahmoudian *et al*., 2018). Additionally, the MMT particle consisted of several layers in which each layer contained two types of structural sheets known as tetrahedral sheet and octahedral sheet (Uddin, 2018). As mentioned by Uddin, the tetrahedral sheet was composed of silicon-oxygen tetrahedra meanwhile the octahedral structure consisted of aluminium or magnesium (Uddin, 2018). Thus, this concluded that the elemental composition of MMT analyzed by EDX was according to the previous literature works as the MMT comprised of main elements such as oxygen, silica and aluminium atoms.

4.2 Membrane Characterization

4.2.1 Fourier Transform Infrared (FTIR) Analysis

The wavelength of the prepared membrane was taken from 4000 – 400 cm^{-1} by focusing to the range of 1700 – 400 cm^{-1}. **Figure 4.4** shows the FTIR spectra of the pristine PSf membrane, 0.5MMM, 1.0MMM and 1.5MMM. It was observed that there were no significant new peaks for MMM as shown in the FTIR spectra due to no chemical interaction involvement between MMT and PSf as reported by Jacob *et al*. (Jacob *et al*., 2020). Furthermore, Singh *et al*. mentioned that there were no significant physical interactions between PSf functional groups and MMT fillers, resulting in no new peaks of MMM in the FTIR spectra (Singh *et al*., 2021). Aside from that, the peaks at 1489 cm^{-1} and 1584 cm^{-1} were corresponding to aromatic C=C stretching meanwhile peaks at 1234 cm^{-1} was attributed to C-O-C stretching (Nasirian *et al*., 2020). Other than that, wavelength at 1301 cm^{-1} represented asymmetric O=S=O stretching whereas wavelength at 1147 cm^{-1} was belongs to symmetric O=S=O stretching (Singh *et al*., 2021). Lastly, the presence of MMT in MMM was validated by the wavelength at 1031 cm^{-1} and 546 cm^{-1} which belongs to Si-O stretching and Al-O-Si deformation accordingly. It was observed as MMT incorporated into the polymer PSf matrix, the transmittance reduced and the peak became smoother as MMT increased as compared to pristine PSf membrane which suggested that the MMT was compatible with the PSf matrix. To summarize, the functional groups presented in both pristine and MMM were aromatic C=C stretching, C-O-C stretching, asymmetric O=S=O stretching and symmetric O=S=O stretching which indicates the sulfone groups, particularly sulphur and oxygen in the PSf matrix whereas the successful employment of MMT in MMM was proven by the presence of Si-O stretching and Al-O-Si deformation.

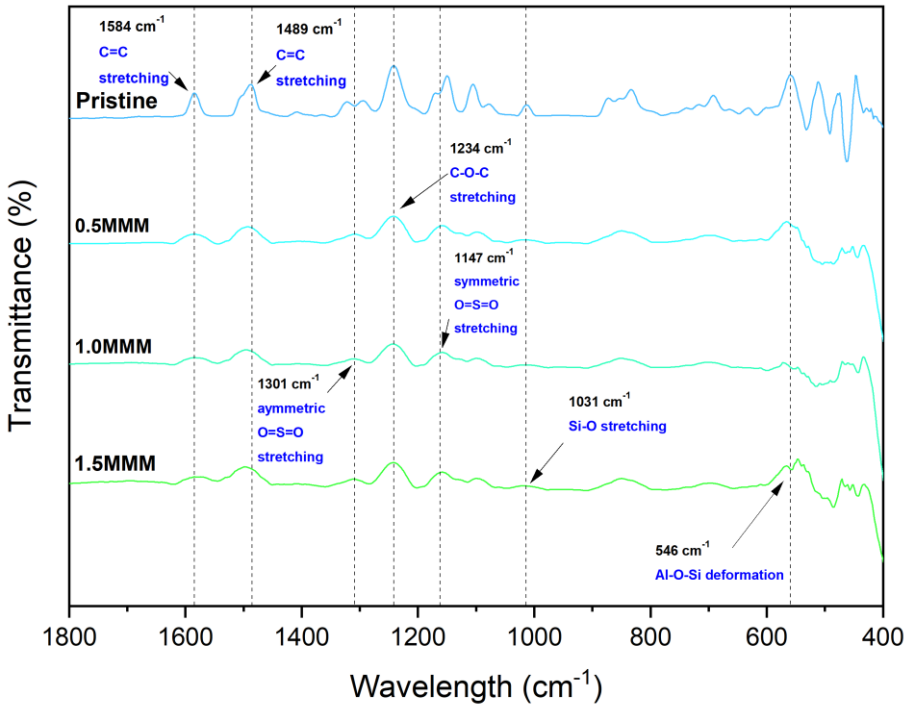

Figure 4.4: FTIR spectra of pristine, 0.5MMM, 1.0MMM and 1.5MMM

4.2.2 Membrane Morphology

The SEM-EDX analysis was conducted at three different spot on the membrane which were cross section, top surface and bottom surface.

4.2.2.1 Membrane Cross Section

The morphology for membrane cross section was taken at 1000 magnification for overall configuration meanwhile membrane cross section at 5000 magnification was taken at top layer and bottom layer of the membrane.

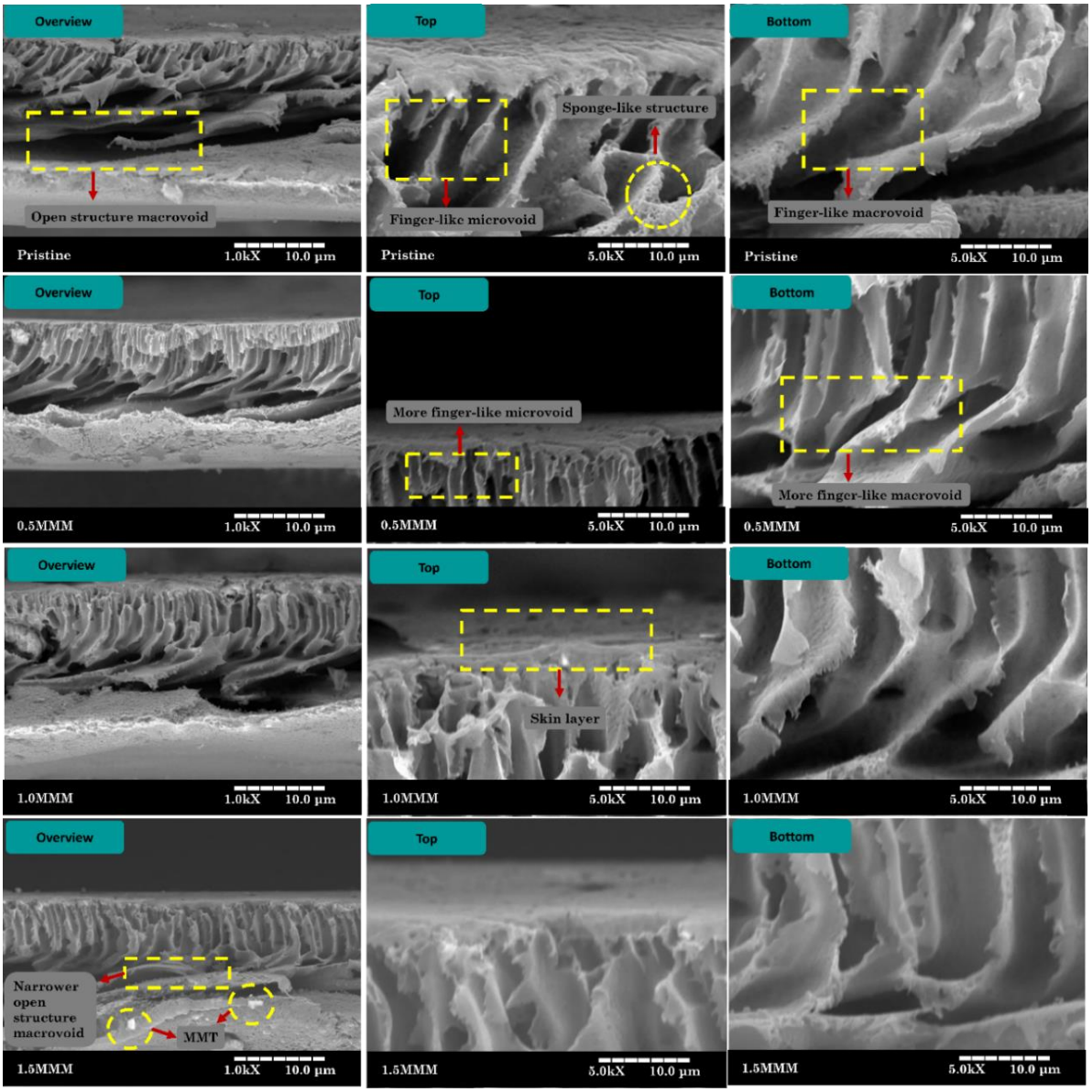

Figure 4.5: Cross section morphology at 1.0 kX for overall view and 5.0 kX magnification at top and bottom views for pristine, 0.5MMM, 1.0MMM and 1.5MMM membranes

Figure 4.5 shows the cross-sectional micrographs of pristine PSf membrane and MMM. Generally, both pristine PSf membrane and MMM had an asymmetric structure across the cross section. There were several characteristics obtained from the membrane cross section including the formation of dense skin layer, finger-like microvoids and macrovoids, open macrovoid structure and porous sponge-like structure. According to Jacob *et al*., the employment of MMT increase the interaction between solvent and nonsolvent, yielding a thinner dense skin layer due to the instantaneous casting solution demixing (Jacob *et al*., 2020).

This can be interpreted that the demixing of instantaneous casting solution had influenced the thickness of the membrane skin layer with the aids of increased interaction between dope solution and MMT as the solvent and nonsolvent respectively. The formation of finger-like microvoids and macrovoids increases as the MMT was employed as compared to the pristine PSf membrane (Ouradi *et al*., 2020). As a result, the increment of finger-like microvoids and macrovoids caused the MMM became denser as the MMT increased. The finger-like macrovoids were discovered larger as MMT loading increases which resulting enhanced the water diffusion flow rate as supported by Ouradi *et al*. (2020). Apart from that, the open structure macrovoids for MMM was observed narrower as compared to pristine PSf membrane (Shokri & Yegani, 2017). For pristine PSf membrane, it was observed that large open structure macrovoids were produced in the sublayer. With the addition of MMT, the size of open structure macrovoids were reduced as illustrated in 0.5 MMM, 1.0MMM and 1.5MMM. According to Shokri & Yegani, the open structure macrovoids were formed due to the low thermodynamic stability and accelerated nucleation from the polymer phase as MMT incorporated into the dope solution (Shokri & Yegani, 2017). Then, a porous sponge-like structure was observed for both pristine PSf membrane and MMM which might to the impact of humidity during the membrane fabrication as suggested as suggested by Khorsand-Ghayeni *et al*., thus there was no significant difference in terms of porous sponge-like structure as the membrane fabrication was conducted at a constant condition. In addition, there were several MMT particles were detected from SEM (Khorsand-Ghayeni *et al*., 2017). This was attributed that the MMT particles were not mixed homogeneously with the dope solution and does not distributed equally across the membrane thickness. Thus, the absence of significant defects in the cross section morphology of MMM was due to excellent adhesion between MMT and PSf matrix. In summary, thinner dense skin layer, increased formation of finger-like microvoids and macrovoids, narrowed open structure macrovoids, unsignificant porous sponge-like structure and increment of white traces as MMT particles were all the observations detected in the prepared membrane as the MMT loading increased.

4.2.2.2 Membrane Top Surface Morphology

The membrane top surface morphology was conducted via SEM at 5000 magnification. **Figure 4.6** illustrates the analysis of top surface images of all membranes including pristine PSf membrane and MMM. The top surface morphology revealed a smooth surface structure

with small open pores. Top surface defects were not obvious for MMM which showed that the MMT and PSf were compatible (Aloisami, 2021). At higher MMT loading percentage, 1.5MMM and 2.0MMM displayed the increment of white traces, indicating that MMT particles obviously protrude in the MMM surface. This was supported by the literature of Bansal *et al*. in which the authors stated that high amount of white traces were due to the interaction between MMT particles, resulting in an increase in viscosity at higher loadings (Bansal *et al*., 2021). Aside from that, hydrophilic MMT act as dispersers of water into small droplets in the surface layer of membranes, which commonly result in a large number of small pore sizes (Dlamini *et al*., 2019). As a result, the top surface morphology for pristine PSf membrane and MMM did not revealed any notable dissimilarity as the formation of pores were uniform as observed at 5000 magnification under SEM. To summarise, the presence of white traces functioned as an indicator for differentiating the top surface structure of pristine PSf membrane from MMM.

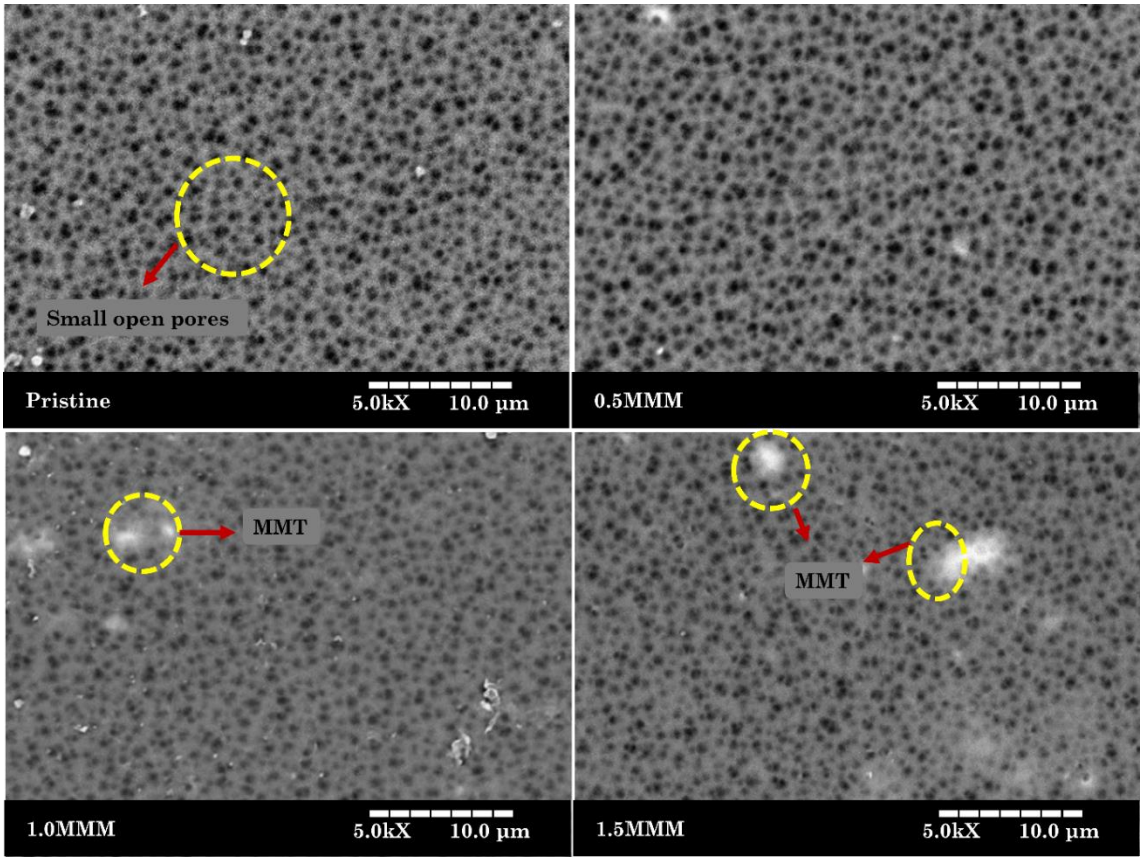

Figure 4.6: Top surface morphology at 5.0 kX magnification for pristine, 0.5MMM, 1.0MMM and 1.5MMM membranes

4.2.2.3 Membrane Bottom Surface Morphology

Figure 4.7 depicted the bottom surface SEM images of pristine PSf membrane and MMM at 500 magnification. For pristine PSf membrane, it was observed that there was a few amount of large asymmetric pores were obtained. In contrast, the number of small pores were enhanced as MMT loading increased. This is due to the preferential wet phase inversion with the incorporation of MMT particles (Simona *et al*., 2017). Besides, Dlamini *et al*. (2019) stated that the ratio increment of MMT inflow to NMP outflow was the main impact to the improved surface porosity which yields a faster separation as MMT was employed to fabricate MMM. Apart from that, as the concentration of MMT increases, more pores were appeared at the membrane's bottom surface, indicating that the finger-like macrovoids were well-connected and penetrating deeper from the top surface to the bottom surface of the membrane. This could create straight routes for water molecules to move through the membrane more efficiently as mentioned by Rastgar *et al*. (2017). In short, the significant observations of membrane's bottom surface were the formation of large number of small pores in which the surface porosity increases as the amount of MMT increased.

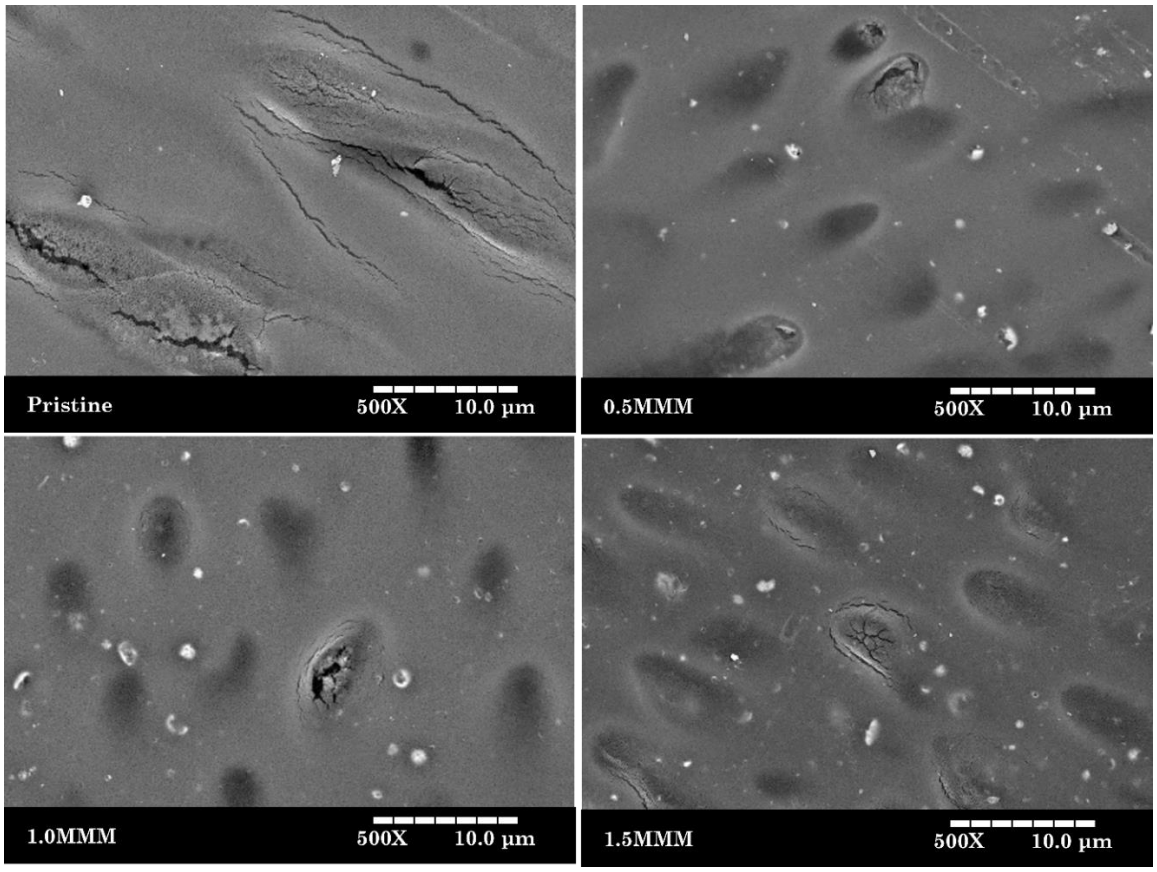

Figure 4.7: Bottom surface morphology at 5.0 kX magnification for pristine, 0.5MMM, 1.0MMM and 1.5MMM membranes

4.2.2.4 Membrane EDX Analysis

The elemental composition of pristine PSf membrane, MMM and MMT for cross section, top surface, and bottom surface under EDX were shown in **Table 4.1**. First and foremost, the EDX elemental composition of pristine PSf membrane for cross section, top surface and bottom surface confirms the presence of carbon, oxygen, and sulphur element which agree well with the elemental composition of the pure PSf matrix (Farrokhara & Dorosti, 2020). For cross section, it was determined that the main elements in MMT including oxygen, silica and aluminium increased up to 1.0MMM. On the other hand, the main element of PSf such as carbon and sulphur decreased up to 1.0MMM.

As for the top surface morphology, oxygen and silica elements increased by 6.85% and 100% respectively whereas carbon elements decreased by 4.79% from pristine to 1.5MMM. Additionally, the mass percentage of the sulphur element showed a mixed pattern. It first declined from pristine to 0.5MMM, then grew from 0.5MMM to 1.0MMM, and then decreased again from 1.0MMM to 1.5MMM. Identically, aluminium had a varied trajectory in terms of mass percentage, with increases from pristine to 0.5MMM, decreases from 0.5MMM to 1.0MMM, and then increases from 1.0MMM to 1.5MMM.

Finally, the bottom surface morphology also showed two patterns in carbon and silica elements, with carbon's mass percentage rising from pristine to 0.5MMM, then falling till 1.5MMM, while sulphur's mass percentage rising from pristine to 0.5MMM, then falling till 1.5MMM. Apart from that, the oxygen element mass percentage increased up to 1.0MMM whereas the mass percentage of silica and aluminium elements increased as MMT increased.

Supposedly, the main elements of MMT and PSf increased as MMT increased which was contradict to the result of EDX analysis since there were several elements that had mixed pattern. This was due to the poor dispersion of MMT in the polymer matrix causing certain cross section, top surface and bottom surface morphology of the MMM had reduced amount of MMT and PSf main elements (Mahmoudian *et al*., 2018). Moreover, the poor dispersion of MMT was proven by particle size distribution result that revealed MMT had wide range of particle size. As mentioned by Maluta *et al*., larger particle size had longer dissolution time (Maluta *et al*., 2019). As a result, there were some large particle size of MMT did not mix

uniformly with the dope solution which might require specific parameters such as increased dissolution time in order to obtain homogenous mixture of dope solution and MMT powder.

Table 4.1: Elemental composition of prepared membrane

Morphology	Element	Mass (wt. %)			
		Pristine	**0.5MMM**	**1.0MMM**	**1.5MMM**
Cross section	Carbon	66.65	64.68	62.67	65.70
	Oxygen	18.90	22.19	23.09	22.92
	Sulphur	10.81	9.43	6.46	7.21
	Sodium	0.29	0	0.27	0
	Silica	0.17	0.50	2.07	0.65
	Aluminium	3.18	3.20	5.24	3.46
	Magnesium	0	0	0.20	0.06
Top surface	Carbon	68.94	67.92	66.51	65.64
	Oxygen	17.55	18.35	18.60	18.84
	Sulphur	12.89	12.36	13.49	11.98
	Sodium	0	0	0	0.19
	Silica	0.10	0.25	0.74	1.71
	Aluminium	0.62	1.12	0.66	1.47
	Magnesium	0	0	0	0.17
Bottom surface	Carbon	68.99	69.06	66.96	66.85
	Oxygen	18.87	19.18	19.50	18.04
	Sulphur	11.75	10.58	11.78	12.28
	Sodium	0	0	0	0
	Silica	0	0.47	0.83	1.73
	Aluminium	0.39	0.65	0.86	1.10
	Magnesium	0	0.06	0.07	0

4.2.3 Water Uptake

As depicted in **Figure 4.8**, it can be evaluated that the water uptake of membrane was increased as the concentration of MMT increased. This was due to the fact that MMT was one

of the clays with hydrophilic properties, which assisted in the transport of water molecules into the membrane structure (Khadhom & Deng, 2019). Moreover, the monovalent ions of MMT which arranged between the layers of silicates tend to attract polar solvent including water as mentioned by Azimi & Peighambardoust (Azimi & Peighambardoust, 2017). In addition, Jacob *et al*. stated that the surface-to-volume ratio of the membrane was improved as the amount of MMT is increased, enhancing the membrane's hydrophilicity (Jacob *et al*., 2020). To summarize, as the MMT loading increases, the water uptake increases as well, which was due to the increased interaction between monovalent MMT ions and water, resulting in an increase in water molecules transfer into the membrane structure. The numerical data as well as detailed calculation of water uptake for each membrane was provided in **Appendix**.

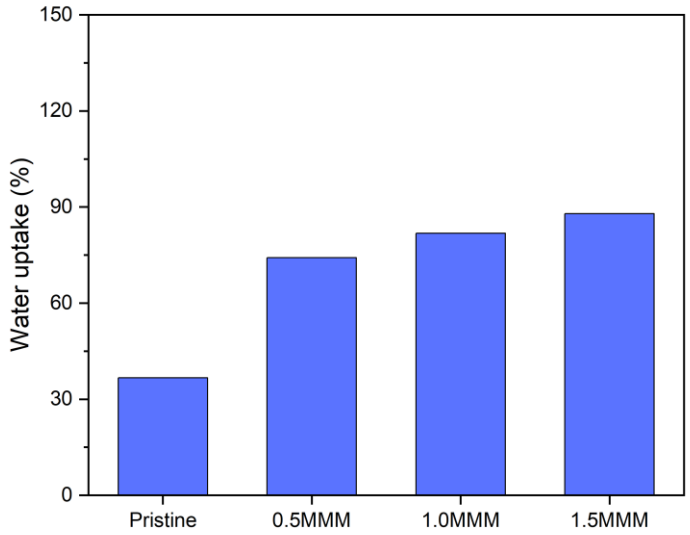

Figure 4.8: Water uptake for pristine, 0.5MMM, 1.0MMM and 1.5MMM membranes

4.3 Membrane Performance

In conducting the membrane performance test, five readings were collected to obtain average reading as well as standard deviation for each membrane. Average reading was necessary to reduce the measurement error whereas standard deviation was crucial to measure the dispersion of data sets around an average. The finalized data of all membrane performance including water uptake, pure water flux and heavy metal rejection were presented in graphical

form using OriginPro 2022 software meanwhile the formulation and calculation of the measured data were computed using Microsoft Excel software.

4.3.1 Pure Water Flux

As shown in **Figure 4.9**, the pure water flux of membrane was enhanced as the MMT loading increased. The detailed calculation of pure water flux was provided in **Appendix** based on membrane effective area of 9.62 cm^2 which required to collect 5mL of permeate. According to Jacob *et al*., the incorporation of MMT's layered structure and hydrophilic characteristics resulted in a significant increase in pure water flux (Jacob *et al*., 2020). Besides, large number of surface porosity of MMM were one of the main reasons that enhanced pure water flux as suggested by Dlamini *et al*. (Dlamini *et al*., 2019). This was related to the SEM morphology of the membrane's bottom surface porosity, which showed that when the MMT concentration increased, the number of surface porosity increased as well. Additionally, Mahmoudian *et al*. stated that the pure water flux of MMM was improved due to the membrane's excellent water holding capacity, efficient water transfer from one side to another side of membrane and the presence of interfacial gaps between layered MMT and the polymer matrix for several additional water pathways (Mahmoudian *et al*., 2018). In summary, as the loading of MMT incorporated into the membrane increases, the high number of surface porosity, excellent water holding capacity of membrane, efficient water transfer from one side to another side of the membrane, and the presence of interfacial gaps between layered MMT and the polymer matrix for several additional water pathways were the main reasons that increased the pure water flux of the membrane.

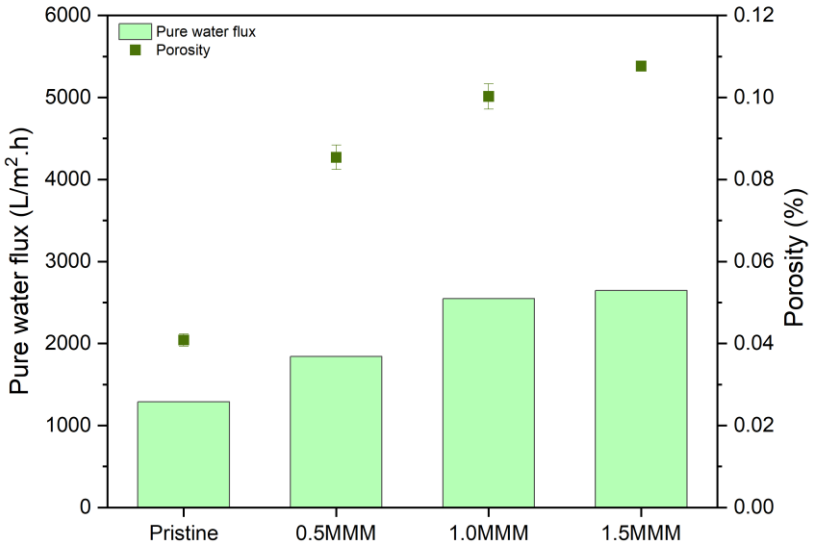

Figure 4.9: Pure water flux for pristine, 0.5MMM, 1.0MMM and 1.5MMM membranes

4.3.2 Heavy Metal Rejection

In this study, cadmium nitrate solution and lead nitrate solution were prepared synthetically to evaluate the heavy metal rejection using prepared membrane including pristine PSf membrane and membrane incorporated with MMT. A 1000 ppm of cadmium and lead were prepared and the solution was diluted using dilution method to obtain standard solution. For cadmium, five standard solution were required which were 0.0 ppm, 0.05 ppm, 0.1 ppm, 0.2 ppm and 0.5 ppm. Identically, five standard solution of lead were prepared which were 0.0 ppm, 0.5 ppm, 1.0 ppm, 2.0 ppm and 5.0 ppm. The function of preparing standard solution was to obtain calibration curve of each heavy metal with R^2 values near to 1. In addition, the standard solution of heavy metal were used along to determine the permeate collected for each membrane. In this analysis, lead and cadmium rejection used 0.5 ppm and 5 ppm, respectively, of the highest standard heavy metal solution when conducting water separation system.

4.3.2.1 Cadmium Rejection

The calibration curves of cadmium was illustrated in **Figure 4.10**. It was observed that the R^2 value of obtained from the calibration curve was 0.9975 which showed a good linearity. This indicates that the correlation between heavy metal concentration and absorbance was good, showing that the AAS equipment was well calibrated as proven by Abidin *et al*. (Abidin *et al*., 2021). High value of R^2 value also indicate that the standard solution for cadmium was well prepared.

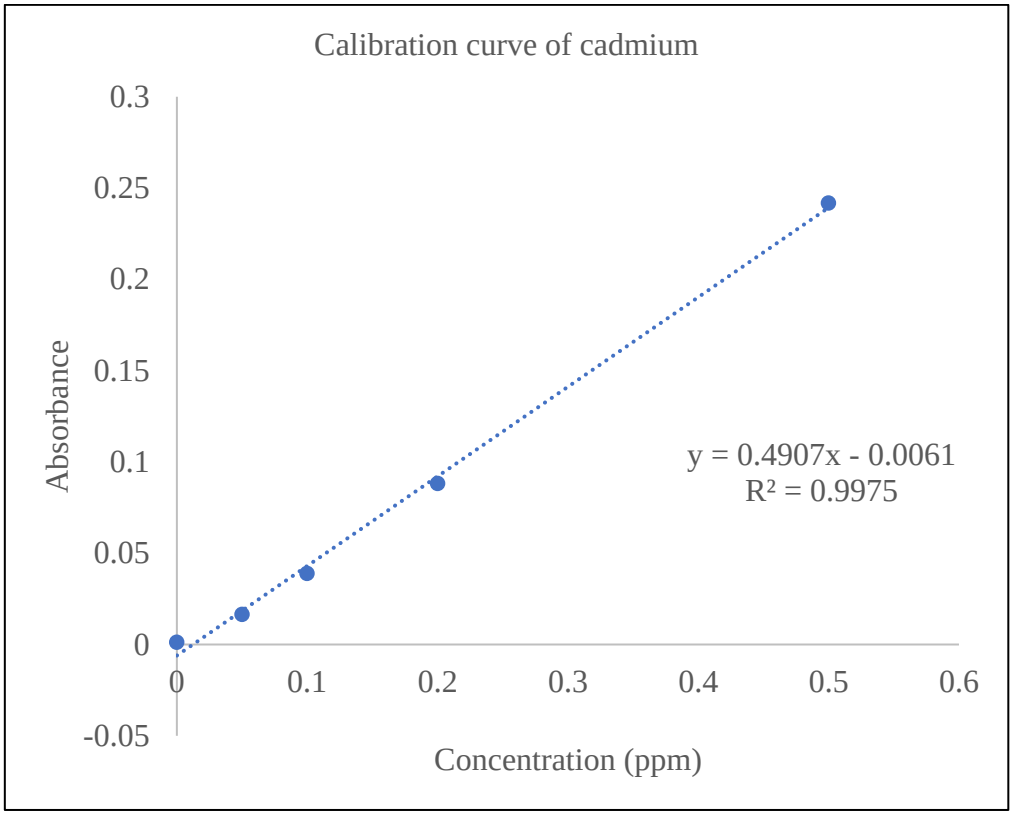

Figure 4.10: Calibration curve of cadmium

Following that, cadmium rejection was depicted in **Figure 4.11**. It can be interpreted that there was no significant trend for cadmium rejection. Moreover, it was observed that there was no rejection of cadmium for 0.5MMM and 1.5MMM. Nonetheless, there was a minimum rejection of cadmium for 1.0MMM with percentage of 3.15% which was lower than the rejection for pristine PSf membrane (4.95%). Supposedly, MMT was employed to improve the performance of pristine PSf membrane. Nevertheless, as MMT incorporated into the PSf matrix, the MMM performance was lower than the pristine PSf membrane. Hence, the MMM

did not provide notable performance in rejecting cadmium in waterways. Since there was no significant rejection of cadmium using MMM, thus another heavy metal which was lead was employed to test the performance of the prepared membrane. On the other hand, the water flux for cadmium was discovered increasing linearly which showed that cadmium rejection was independent to water flux. The increased of cadmium water flux was due to the membrane bottom surface SEM morphology as illustrated in **Figure 4.7** earlier that the bottom surface porosity was increased as MMT loading increased. Consequently, additional solution pathways at bottom surface porosity was enhanced causing increased water flux of cadmium.

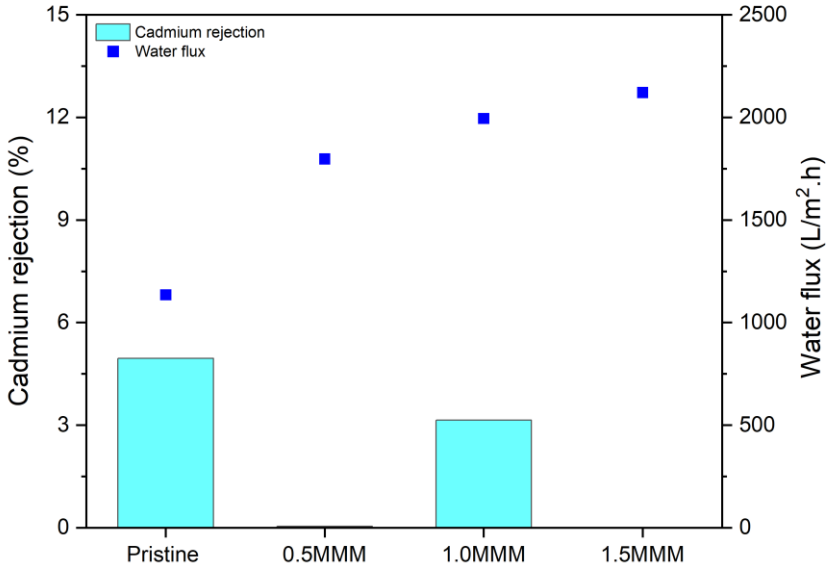

Figure 4.11: Cadmium rejection

4.3.2.2 Lead Rejection

The calibration curves of lead was illustrated in **Figure 4.12** with R^2 value of 0.9987. Since the R^2 was near to 1, thus the value indicates that the standard solution of lead were prepared properly and the correlation between heavy metal concentration and absorbance was good as identical to cadmium calibration curve. The standard solution of lead were used along

to determine the concentration of permeate collected for each membrane using AAS equipment.

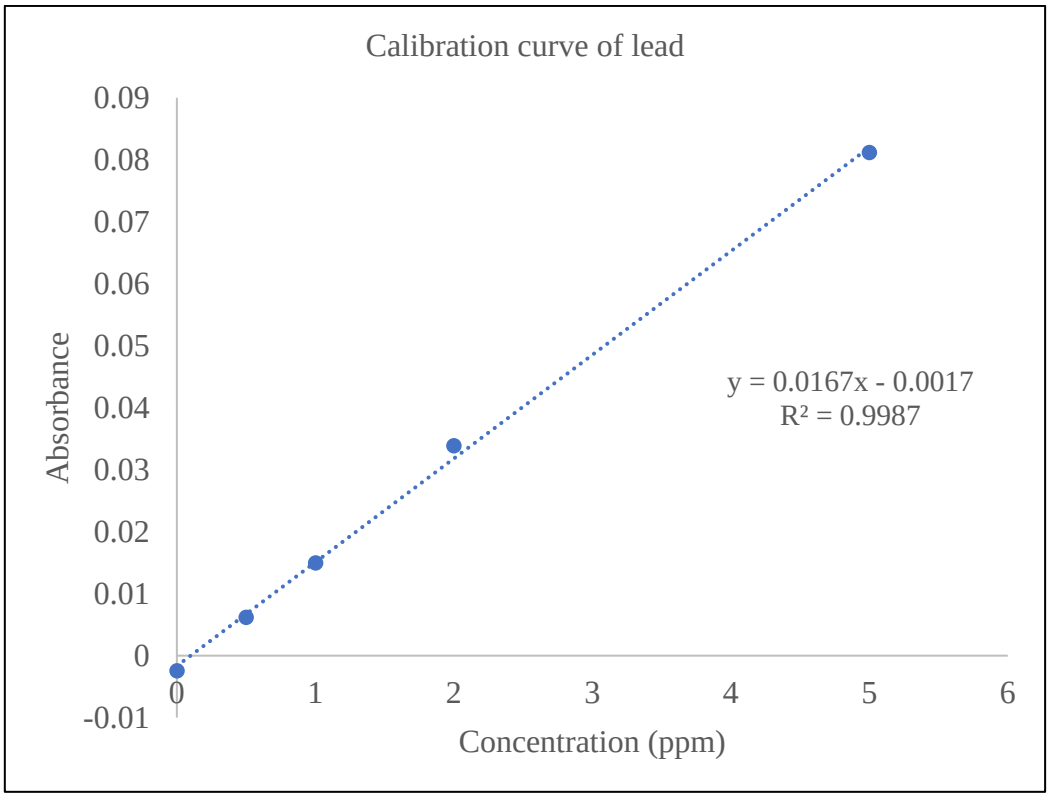

Figure 4.12: Calibration curve of lead

For lead rejection as illustrated in **Figure 4.13**, an increasing pattern was obtained from pristine PSf membrane to 0.5MMM then the trend was fall as MMT loading was increased, particularly 1.0MMM and 1.5MMM. Besides, it can be seen that the highest lead rejection is at 0.5% of MMT loading (0.5MMM), yielding 14.36% rejection. Then, the lead rejection was reduced as the concentration of MMT above 0.5%. One of the primary causes of reduced lead rejection was due to the agglomeration of MMT as higher loading of MMT was employed (Kord *et al*., 2017). Although the bottom surface porosity exhibited in earlier SEM morphology (**Figure 4.7**) revealed higher surface porosity as MMT increased, the aggregates of MMT may obstruct the membrane pores, resulting in a reduction in the effective membrane surface area. The blockage of membrane pores due to nanoclay agglomeration was according to the study of Jacob *et al*. (Jacob *et al*., 2020). Moreover, the addition of pressure from water flow in the water separation system along with pore blockage aids in the surface defects of MMM results

from the agglomeration of MMT. As reported by Vu *et al*., the agglomeration of nanoclay particles can lead to the formation of surface defects such as holes on the membrane, resulting the decline of heavy metal rejection (Vu *et al*., 2021).

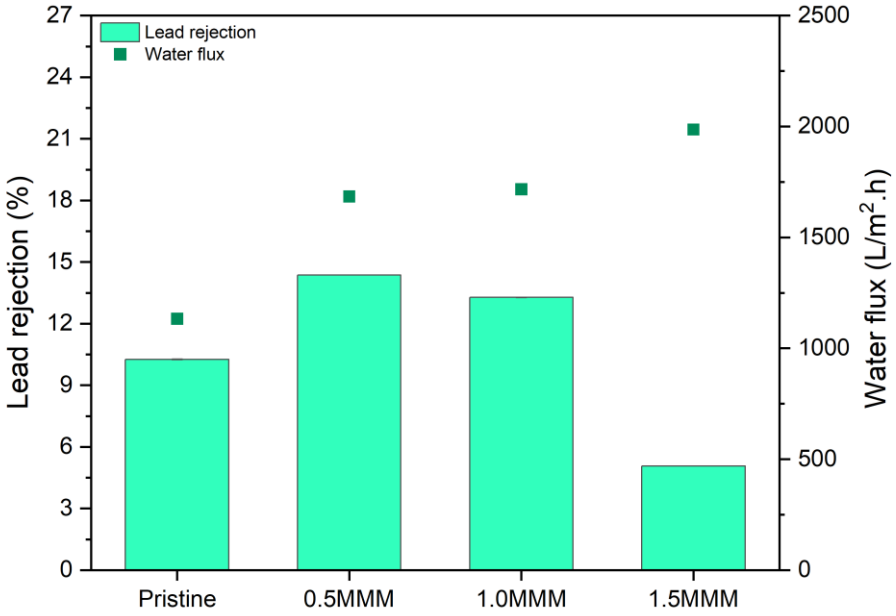

Figure 4.13: Lead rejection

4.3.2.3 Comparison between Cadmium and Lead Rejection

One of the main reasons that contribute to the effectiveness of heavy metal rejection trend was the wide range of MMT particle size distribution as studied previously in MMT characterization via PSA Based on the PSA result, it showed that MMT does not have consistent particle size which cause the aggregation of MMT. This was proven by the study of Tan *et al*. that reported the aggregation of clay minerals was due to low stability of clay mineral dispersion (Tan *et al*., 2017). Besides, MMT had poor dispersion as it tends to agglomerate, causing the membrane performance in terms of selectivity to be decreased (Mahmoudian *et al*., 2018). Hence, lower range of particle size for MMT was required to reduce the aggregation of MMT so that the particles were distributed equally across the PSf matrix.

Besides, the particle size of heavy metal also contributes to the performance of heavy metal rejection. As mentioned earlier in the background of heavy metals, cadmium had approximate average particle size of 0.075μm (Vadagama *et al*., 2017). On the other hand, the approximate average particle size of lead was 1μm (Matthew & Krishnamurthy, 2018). Since cadmium had smaller particle size than lead, thus cadmium able to pass through the membrane easily, yielding unsignificant rejection and obtained higher permeate flux than lead when conducting water separation system. Therefore, it was crucial to determine the pore size of the membrane which became the limitation of this study since the pore size produced were asymmetric shape and different for each membrane.

Finally, the comparison of permeate flux between cadmium and lead was conducted. It can be seen that the permeate flux for cadmium was higher than lead permeate flux. As stated earlier, the particle size of lead was higher than cadmium, thus the larger particle size of lead hindered the flow of solution throughout the water separation system. This was supported by the study of Ramli *et al*. as the authors mentioned that larger particle size cause the blockage of membrane pores which reduced the permeate flux due the cake layer formation (Ramli *et al*., 2020). Hence, the permeate flux for lead was lower than the cadmium. Overall, the permeate flux for both cadmium and lead increased as the concentration of MMT increases due to additional solution pathways as bottom surface porosity was enhanced with the addition of MMT agglomeration occurrence that caused the formation of tiny holes on the membrane as the MMT loading increased.

4.4 Summary

In a nutshell, the characterization of MMT were conducted via PSA, FTIR, and SEM-EDX analysis. Apart from that, the FTIR and SEM-EDX analysis were employed to evaluate the membrane characterization. The SEM-EDX analysis for the prepared membrane was conducted for three morphologies including membrane cross section, membrane top surface and membrane bottom surface. Then, the prepared membrane were characterized in terms of its water uptake to evaluate the membrane capability to absorb water. Finally, the membrane performance was executed in terms of pure water flux and heavy metal rejection. Based on the membrane performance, as the MMT loading increased, the pure water flux of the prepared membrane were also increased. As for heavy metal rejection test, the calibration curves for

cadmium and lead demonstrated a good correlation between heavy metal concentration and absorbance with R^2 values greater than 0.99. It was observed that minimum cadmium rejection was obtain for 1.0MMM meanwhile lead rejection showed monomodal pattern with highest rejection at 0.5MMM, yielding 14.36% rejection. Next, the permeate flux for cadmium and lead were increasing linearly. To conclude, 1.0MMM was the most preferred MMM as it has significant rejection of cadmium and lead as well as higher water uptake, pure water flux, surface porosity and permeate flux.

CHAPTER 5

CONCLUSION & RECOMMENDATION

5.1 Conclusion

In summary, the background of study for heavy metals, wastewater treatment via membrane technology, polymeric membrane, and MMT are presented. Besides, the issues regarding the utilisation of polymeric membrane as well as inorganic membrane are described. The research questions, objectives, scopes of study and expected results are also considered.

Following that, there is an extensive research on heavy metal removal that includes the negative effects on public health, the allowed limit, and particle size. The principles of membrane filtering mechanisms are covered, as well as an in-depth overview of the most often employed organic and inorganic membranes. In addition, the evaluation of various forms of layer silicates clay minerals is thoroughly examined. The literature on MMM fabrication is assessed in terms of the different types of organic and inorganic membranes, membrane mechanisms, water flux, heavy metal types and concentrations, removal capability, and the membrane's advantages and disadvantages. Aside from that, the benefits and drawbacks of various membrane fabrication techniques are presented.

In this study, the MMM comprised of PSf and MMT is fabricated by using phase inversion technique to remove copper and lead. Then, the MMT and prepared membrane are characterized in terms chemical and physical properties. For chemical properties of MMT and prepared membrane, both are analyzed by using FTIR. On the other hand, the physical properties of MMT is evaluated by using PSA and SEM-EDX meanwhile the physical properties of the prepared membrane is investigated by using SEM-EDX. The membrane performance, on the other hand, were analyzed in terms of water uptake, pure water flux and heavy metal rejection. The prepared membrane were tested by using water separation system

to evaluate the pure water permeability and capability of the membrane to remove heavy metal in water.

Based on the characterization of MMT, PSA revealed that the particle size of MMT was monomodal distribution with a mean diameter of 13.21μm and the sizes of most of the MMT particles lie within a wide range of 1.60μm to 45.0μm. As for FTIR, there were several functional groups observed for MMT including O-H stretching, O-H bending, Si-O stretching, Al-OH-Al bending and Si-O bending. Following that, the SEM analysis showed that MMT particles had several significant characteristics including irregular shape and polydisperse pattern that agglomerates whereas EDX analysis evaluated that the MMT comprised of main elements such as oxygen, silica and aluminium atoms due to high mass percentage.

Apart from that, FTIR analysis for prepared membrane displayed that the FTIR spectra of pristine PSf membrane and MMM were almost identical due to no obvious physical and chemical interaction involvement between MMT and PSf. The functional groups for the prepared membrane includes C=C stretching, C-O-C stretching, asymmetric O=S=O stretching and symmetric O=S=O stretching in which the presence of MMT in MMM was validated by the functional group Si-O bending. Following that, the SEM-EDX analysis for the prepared membrane was conducted for three morphologies including membrane cross section, membrane top surface and membrane bottom surface. There were several characteristics obtained from the membrane cross section such as the formation of dense skin layer, finger-like microvoids and macrovoids, open macrovoid structure and porous sponge-like structure. As for membrane top surface morphology, a smooth surface structure with small open pores were observed for all of the prepared membrane. Then, the formation of asymmetric pores were seen at the bottom surface morphology and became enhanced as the concentration of MMT increased. Other than that, the elemental composition of the prepared membrane for all of the morphologies including cross section, top surface and bottom surface were determined via EDX analysis. It was found that there were several main elements of MMT and PSf had mixed trend due to the poor dispersion of MMT in the polymer matrix as well as wide particle size range causing certain cross section, top surface and bottom surface morphology of the MMM had reduced amount of MMT and PSf main elements. Lastly, water uptake analysis was included in membrane characterization in which the water uptake of the prepared membrane increased as MMT loading increased.

The membrane performance was executed in terms of pure water flux and heavy metal rejection. Based on the membrane performance, as the MMT loading increased, the pure water flux of the prepared membrane were also increased. Finally, heavy metal rejection using prepared membrane was evaluated by using cadmium and lead as heavy metal. The calibration curves for cadmium and lead obtained R^2 values were greater than 0.99 which demonstrated a good linearity as well as good correlation between heavy metal concentration and absorbance due to well calibrated AAS equipment. It can be interpreted that there was no significant trend for cadmium rejection in which there was minimum rejection at 1.0MMM. In contrast, lead rejection showed monomodal pattern with highest rejection at 0.5MMM, yielding 14.36% rejection. Next, the permeate flux for cadmium and lead were conducted as well and the results showed that permeate flux for both heavy metals increased as the concentration of MMT increases. The standard deviation was also evaluated for each membrane performance. Overall, the standard deviation of data collected for each sample was low indicating that the data were clustered closely around the mean which made the data were reliable. To conclude, 1.0MMM was the most preferred MMM as it has significant rejection of cadmium and lead as well as higher pure water flux, surface porosity and permeate flux.

5.2 Recommendations

There were several recommendations were suggested for the future works of this project. First and foremost, membrane characterization such as Brunauer-Emmet-Teller (BET) analysis can be employed to determine the porosity and surface area of the prepared membrane. According to Virtanen *et al.*, porosity and surface area are important factors in membrane research since they disclose the membrane's structural features and may even reveal potential foulant accumulation spots (Virtanen *et al*., 2020). Besides, Abd-Razak *et al*. utilized BET analysis to prosity measurement including the total pore areas and volumes of the membrane that affect the membrane fouling (Abd-Razak *et al*., 2021). Hence, the BET analysis aids in the study of membrane fouling.

In addition, the membrane antifouling property can be studied to evaluate the membrane performance in terms membrane blocking mechanism during the filtration of heavy metal

solution utilising prepared membrane (Abd Hamid *et al*., 2021). This can be achieved by testing the produced membrane's antifouling properties using foulant such as Bovine Serum Albumin (BSA) flow tests. Apart from that, humic acid also can be applied as foulant to determine the antifouling properties of the prepared membrane by measuring the flux recovery ratio as suggected by Lavanya *et al*. (Lavanya *et al*., 2019). Thus, the performance of membrane in terms of antifouling properties can be evaluated for the future work.

Last but not least, the PSA characterization of clay particles can be improved in the future. In this study, the particle size distribution of clay had wide range of particle sizes. Wide particle size of clay cause inconsistent in producing MMM. Therefore, sieving of MMT powders can be applied to obtain smaller range of clay particle size as well as reduced the aggregation of particles as studied by Tan *et al*. (Tan *et al*., 2017). Moreover, sieving leads to an increased limit as more clay able to hold more water molecules during the fabrication of membrane as mentioned by Won *et al*. (Won *et al*., 2021). To conclude, the particle size of clay such as MMT in this project had significant impact to the performance of the prepared membrane.

REFERENCES

Abd Hamid, S., Shahadat, M., & Ismail, S. (2021). Zeolite–polysulfone-based adsorptive membrane for removal of metal pollutants. *Chemical Papers*, 1-14.

Abdel-Karim, A., El-Naggar, M. E., Radwan, E. K., Mohamed, I. M., Azaam, M., & Kenawy, E. R. (2021). High-performance mixed-matrix membranes enabled by organically/inorganic modified montmorillonite for the treatment of hazardous textile wastewater. *Chemical Engineering Journal*, *405*, 126964.

Abd-Razak, N. H., Pihlajamäki, A., Virtanen, T., Chew, Y. J., & Bird, M. R. (2021). The influence of membrane charge and porosity upon fouling and cleaning during the ultrafiltration of orange juice. *Food and Bioproducts Processing*, *126*, 184-194.

Abdullah, N., Yusof, N., Lau, W. J., Jaafar, J., & Ismail, A. F. (2019). Recent trends of heavy metal removal from water/wastewater by membrane technologies. *Journal of Industrial and Engineering Chemistry*, *76*, 17-38.

Abetz, V., Brinkmann, T., & Sözbilir, M. (2021). Fabrication and function of polymer membranes. *Chemistry Teacher International*.

Abidin, N. A. Z., Kassim, N. S. A. K., Izzadin, S. A., Ghazali, S. M., Pungot, N. H., & Kamni, S. S. (2021). Evaluation of Heavy Metals Concentration in Milk Products by using Atomic Absorption Spectroscopy. *EKSAKTA: Journal of Sciences and Data Analysis*, *2*(2), 136-141.

Alekseeva, O., Noskov, A., Grishina, E., Ramenskaya, L., Kudryakova, N., Ivanov, V., & Agafonov, A. (2019). Structural and thermal properties of montmorillonite/ionic liquid composites. *Materials*, *12*(16), 2578.

Alenazi, N. A., Hussein, M. A., Alamry, K. A., & Asiri, A. M. (2017). Modified polyether-sulfone membrane: a mini review. *Designed monomers and polymers*, *20*(1), 532-546.

Alqaheem, Y., & Alomair, A. A. (2020). Microscopy and Spectroscopy Techniques for Characterization of polymeric membranes. *Membranes*, *10*(2), 33.

AlSawaftah, N., Abuwatfa, W., Darwish, N., & Husseini, G. (2021). A Comprehensive Review on Membrane Fouling: Mathematical Modelling, Prediction, Diagnosis, and Mitigation. *Water*, *13*(9), 1327.

Asad, A., Sameoto, D., & Sadrzadeh, M. (2020). Overview of membrane technology. In *Nanocomposite Membranes for Water and Gas Separation* (pp. 1-28). Elsevier.

Ashiq, A., Sarkar, B., Adassooriya, N., Walpita, J., Rajapaksha, A. U., Ok, Y. S., & Vithanage, M. (2019). Sorption process of municipal solid waste biochar-montmorillonite composite for ciprofloxacin removal in aqueous media. *Chemosphere*, *236*, 124384.

Azimi, A., Azari, A., Rezakazemi, M., & Ansarpour, M. (2017). Removal of heavy metals from industrial wastewaters: a review. *ChemBioEng Reviews*, *4*(1), 37-59.

Azimi, M., & Peighambardoust, S. J. (2017). Methanol crossover and selectivity of nafion/heteropolyacid/montmorillonite nanocomposite proton exchange membranes for DMFC Applications. *Iranian Journal of Chemical Engineering (IJChE)*, *14*(3), 65-81.

Bansal, P., Batra, R., Yadav, R., & Purwar, R. (2021). Electrospun polyacrylonitrile nanofibrous membranes supported with montmorillonite for efficient PM2. 5 filtration and adsorption of Cu (II) ions. *Journal of Applied Polymer Science*, 51582.

Barakan, S., & Aghazadeh, V. (2019). Separation and characterisation of montmorillonite from a low-grade natural bentonite: using a non-destructive method. *Micro & Nano Letters*, *14*(6), 688-693.

Bee, S. L., Abdullah, M. A. A., Bee, S. T., Sin, L. T., & Rahmat, A. R. (2018). Polymer nanocomposites based on silylated-montmorillonite: A review. *Progress in Polymer Science*, *85*, 57-82.

Bourdelle, F. (2021). Low-temperature chlorite geothermometry and related recent analytical advances: a review. *Minerals*, *11*(2), 130.

Brame, J. A., & Griggs, C. S. (2016). Surface area analysis using the Brunauer-Emmett-Teller (BET) method: scientific operation procedure series: SOP-C.

Caccamo, M. T., Mavilia, G., Mavilia, L., Lombardo, D., & Magazù, S. (2020). Self-assembly processes in hydrated montmorillonite by FTIR investigations. *Materials*, *13*(5), 1100.

Castellini, E., Malferrari, D., Bernini, F., Brigatti, M. F., Castro, G. R., Medici, L., ... & Borsari, M. (2017). Baseline studies of the clay minerals society source clay montmorillonite stx-1b. *Clays and Clay Minerals*, *65*(4), 220-233.

Centeri, C., Jakab, G. I., Szabó, S., Farsang, A., Barta, K., Szalai, Z., & Bíró, Z. (2015). Comparison of particle-size analyzing laboratory methods. *Environmental Engineering and Management Journal*, *14*(5), 1125-1135.

Chai, W. S., Cheun, J. Y., Kumar, P. S., Mubashir, M., Majeed, Z., Banat, F., ... & Show, P. L. (2021). A review on conventional and novel materials towards heavy metal adsorption in wastewater treatment application. *Journal of Cleaner Production*, *296*, 126589.

Chandrashekhar, N., Isloor, A. M., Lakshmi, B., Marwani, H. M., & Khan, I. (2019). Polyphenylsulfone/multiwalled carbon nanotubes mixed ultrafiltration membranes: Fabrication, characterization and removal of heavy metals Pb2+, Hg2+, and Cd2+ from aqueous solutions.

Cheng, Y., Ying, Y., Japip, S., Jiang, S. D., Chung, T. S., Zhang, S., & Zhao, D. (2018). Advanced porous materials in mixed matrix membranes. *Advanced Materials*, *30*(47), 1802401.

Crini, G., & Lichtfouse, E. (2019). Advantages and disadvantages of techniques used for wastewater treatment. *Environmental Chemistry Letters*, *17*(1), 145-155.

Czarnecka-Komorowska, D., Grześkowiak, K., Popielarski, P., Barczewski, M., Gawdzińska, K., & Popławski, M. (2020). Polyethylene wax modified by organoclay bentonite used in the lost-wax casting process: processing− structure− property relationships. *Materials*, *13*(10), 2255.

Delavar, M., Bakeri, G., & Hosseini, M. (2017). Fabrication of polycarbonate mixed matrix membranes containing hydrous manganese oxide and alumina nanoparticles for heavy metal decontamination: characterization and comparative study. *Chemical Engineering Research and Design*, *120*, 240-253.

Dickhout, J. M., Moreno, J., Biesheuvel, P. M., Boels, L., Lammertink, R. G. H., & De Vos, W. M. (2017). Produced water treatment by membranes: a review from a colloidal perspective. *Journal of colloid and interface science*, *487*, 523-534.

Dlamini, D. S., Li, J., & Mamba, B. B. (2019). Critical review of montmorillonite/polymer mixed-matrix filtration membranes: Possibilities and challenges. *Applied Clay Science*, *168*, 21-30.

Dong, X., Lu, D., Harris, T. A., & Escobar, I. C. (2021). Polymers and Solvents Used in Membrane Fabrication: A Review Focusing on Sustainable Membrane Development. *Membranes*, *11*(5), 309.

Dutta, M., Jana, A., & De, S. (2021). Insights to the transport of heavy metals from an industrial effluent through functionalized bentonite incorporated mixed matrix membrane: Process modeling and analysis of the interplay of various parameters. *Chemical Engineering Journal*, *413*, 127397.

Farrokhara, M., & Dorosti, F. (2020). New high permeable polysulfone/ionic liquid membrane for gas separation. *Chinese Journal of Chemical Engineering*, *28*(9), 2301-2311.

Fulignati, P. (2020). Clay minerals in hydrothermal systems. *Minerals*, *10*(10), 919.

Hebbar, R. S., Isloor, A. M., Prabhu, B., Asiri, A. M., & Ismail, A. F. (2018). Removal of metal ions and humic acids through polyetherimide membrane with grafted bentonite clay. *Scientific reports*, *8*(1), 1-16.

Jacob, L., Joseph, S., & Varghese, L. A. (2020). Polysulfone/MMT mixed matrix membranes for hexavalent chromium removal from wastewater. *Arabian Journal for Science and Engineering*, *45*(9), 7611-7620.

Judd, S. J. (2017). Membrane technology costs and me. *Water research* 122 (2017): 1-9.

Kadhom, M., & Deng, B. (2019). Thin film nanocomposite membranes filled with bentonite nanoparticles for brackish water desalination: A novel water uptake concept. *Microporous and Mesoporous Materials*, *279*, 82-91.

Kayvani Fard, A., McKay, G., Buekenhoudt, A., Al Sulaiti, H., Motmans, F., Khraisheh, M., & Atieh, M. (2018). Inorganic membranes: Preparation and application for water treatment and desalination. *Materials*, *11*(1), 74.

Kheirieh, S., Asghari, M., & Afsari, M. (2018). Application and modification of polysulfone membranes. *Reviews in Chemical Engineering*, *34*(5), 657-693.

Khorsand-Ghayeni, M., Barzin, J., Zandi, M., & Kowsari, M. (2017). Fabrication of asymmetric and symmetric membranes based on PES/PEG/DMAc. *Polymer Bulletin*, *74*(6), 2081-2097.

Kinuthia, G. K., Ngure, V., Beti, D., Lugalia, R., Wangila, A., & Kamau, L. (2020). Levels of heavy metals in wastewater and soil samples from open drainage channels in Nairobi, Kenya: community health implication. *Scientific Reports*, *10*(1), 1-13.

Kord, B., Ravanfar, P., & Ayrilmis, N. (2017). Influence of organically modified nanoclay on thermal and combustion properties of bagasse reinforced HDPE nanocomposites. *Journal of Polymers and the Environment*, *25*(4), 1198-1207.

Kumari, N., & Mohan, C. (2021). Basics of clay minerals and their characteristic properties. In *Clay and Clay Minerals*. IntechOpen.

Kurakula, M., & Rao, G. K. (2020). Type of Article: REVIEW Pharmaceutical Assessment of Polyvinylpyrrolidone (PVP): As Excipient from Conventional to Controlled Delivery Systems with a Spotlight on COVID-19 Inhibition. *Journal of Drug Delivery Science and Technology*, 102046.

Ladewig, B., & Al-Shaeli, M. N. Z. (2017). Fundamentals of membrane bioreactors. *Springer Transactions in Civil and Environmental Engineering*.

Lavanya, C., Balakrishna, R. G., Soontarapa, K., & Padaki, M. S. (2019). Fouling resistant functional blend membrane for removal of organic matter and heavy metal ions. *Journal of environmental management*, *232*, 372-381.

Li, S., Tao, Q., Ma, L., Zhang, C., Yang, Y., Du, P., ... & Zhu, J. (2021). Release of mg and fe from the Octahedral Sheets during the Transformation of Montmorillonite Into Kaolinite. *Clays and Clay Minerals*, *69*(4), 453-462.

Liao, Y., Loh, C. H., Tian, M., Wang, R., & Fane, A. G. (2018). Progress in electrospun polymeric nanofibrous membranes for water treatment: Fabrication, modification and applications. *Progress in Polymer Science*, *77*, 69-94.

Liu, R., Li, S., Otitoju, T. A., Wang, S., Zhang, A., & Zhang, L. (2021). Exfoliation of montmorillonite using a simple and low-cost heating/gasifying method. *Applied Nanoscience*, *11*(4), 1427-1436.

Liu, X., Zhou, F., Chi, R., Feng, J., Ding, Y., & Liu, Q. (2019). Preparation of modified montmorillonite and its application to rare earth adsorption. *Minerals*, *9*(12), 747.

Liu, Y., Shen, D., Chen, G., Elzatahry, A. A., Pal, M., Zhu, H., ... & Zhao, D. (2017). Mesoporous silica thin membranes with large vertical mesochannels for nanosize-based separation. *Advanced Materials*, *29*(35), 1702274.Ying, Y. P., Kamarudin, S. K., & Masdar, M. S. (2018). Silica-related membranes in fuel cell applications: An overview. *International Journal of Hydrogen Energy*, *43*(33), 16068-16084.

Maddah, H. A., Alzhrani, A. S., Bassyouni, M., Abdel-Aziz, M. H., Zoromba, M., & Almalki, A. M. (2018). Evaluation of various membrane filtration modules for the treatment of seawater. *Applied Water Science*, *8*(6), 1-13.

Madhav, S., Ahamad, A., Singh, A. K., Kushawaha, J., Chauhan, J. S., Sharma, S., & Singh, P. (2020). Water pollutants: sources and impact on the environment and human health. In *Sensors in Water Pollutants Monitoring: Role of Material* (pp. 43-62). Springer, Singapore.

Mahmoudian, M., Balkanloo, P. G., & Nozad, E. (2018). A facile method for dye and heavy metal elimination by pH sensitive acid activated montmorillonite/polyethersulfone nanocomposite membrane. *Chinese Journal of Polymer Science*, *36*(1), 49-57.

Maluta, F., Montante, G., & Paglianti, A. (2019). Analyis of liquid mixing and solid dissolution for pharmaceutical manufacturing in stirred tanks. *Chemical Engineering Transactions*, *74*, 949-954.

Massaro, M., Colletti, C. G., Lazzara, G., & Riela, S. (2018). The use of some clay minerals as natural resources for drug carrier applications. *Journal of functional biomaterials*, *9*(4), 58.

Mathew, B. B., & Krishnamurthy, N. B. (2018). Evaluation of lead oxide nanoparticles synthesized by chemical and biological methods. *Journal of Nanomedicine Research*, *7*(3), 195-198.

Mondal, M., Dutta, M., & De, S. (2017). A novel ultrafiltration grade nickel iron oxide doped hollow fiber mixed matrix membrane: Spinning, characterization and application in heavy metal removal. *Separation and Purification Technology*, *188*, 155-166.

Muharrem, I. N. C. E., & Ince, O. K. (2017). An overview of adsorption technique for heavy metal removal from water/wastewater: a critical review. *International Journal of Pure and Applied Sciences*, *3*(2), 10-19.

Nadziakiewicza, M., Kehoe, S., & Micek, P. (2019). Physico-chemical properties of clay minerals and their use as a health promoting feed additive. *Animals*, *9*(10), 714.

Nasirian, D., Salahshoori, I., Sadeghi, M., Rashidi, N., & Hassanzadeganroudsari, M. (2020). Investigation of the gas permeability properties from polysulfone/polyethylene glycol composite membrane. *Polymer Bulletin*, *77*(10), 5529-5552.

Natarajan, P., Sasikumar, B., Elakkiya, S., Arthanareeswaran, G., Ismail, A. F., Youravong, W., & Yuliwati, E. (2021). Pillared cloisite 15A as an enhancement filler in polysulfone mixed matrix membranes for CO2/N2 and O2/N2 gas separation. *Journal of Natural Gas Science and Engineering*, *86*, 103720.

Nazir, L. S. M., Yeong, Y. F., & Chew, T. L. (2020). Methods and synthesis parameters affecting the formation of FAU type zeolite membrane and its separation performance: a review. *Journal of Asian Ceramic Societies*, *8*(3), 553-571.

Nqombolo, A., Mpupa, A., Moutloali, R. M., & Nomngongo, P. N. (2018). Wastewater treatment using membrane technology. *Wastewater and Water Quality*, *29*.

Obotey Ezugbe, E., & Rathilal, S. (2020). Membrane technologies in wastewater treatment: a review. *Membranes*, *10*(5), 89.

Olopade, B. K., Oranusi, S. U., Nwinyi, O. C., Njobeh, P. B., & Lawal, I. A. (2019, December). Studies on FT-IR Spectroscopy of modified Montmorillonite clays applied for the removal of T-2 toxin in maize. In *Journal of Physics: Conference Series* (Vol. 1378, No. 2, p. 022065). IOP Publishing.

Ouardi, L. M., Laabd, M., Abou Oualid, H., Brahmi, Y., Abaamrane, A., Elouahli, A., ... & Laknifli, A. (2019). Efficient removal of p-nitrophenol from water using montmorillonite clay: insights into the adsorption mechanism, process optimization, and regeneration. *Environmental Science and Pollution Research*, *26*(19), 19615-19631.

Ouradi, A., Cherifi, N., Nguyen, Q. T., & Benaboura, A. (2020). Preliminary study of the prepared polysulfone/AN69/clay composite membranes intended for the hemodialysis application. *Chemical Papers*, *74*(7), 2133-2144.

Perelomov, L., Mandzhieva, S., Minkina, T., Atroshchenko, Y., Perelomova, I., Bauer, T., ... & Barakhov, A. (2021). The Synthesis of Organoclays Based on Clay Minerals with Different Structural Expansion Capacities. *Minerals*, *11*(7), 707.

Pérez-Tello, M., Parra-Sánchez, V. R., Sánchez-Corrales, V. M., Gómez-Álvarez, A., Brown-Bojórquez, F., Parra-Figueroa, R. A., ... & Araneda-Hernández, E. A. (2018). Evolution of size and chemical composition of copper concentrate particles oxidized under simulated flash smelting conditions. *Metallurgical and Materials Transactions B*, *49*(2), 627-643.

Qadir, D., Mukhtar, H., & Keong, L. K. (2017). Mixed matrix membranes for water purification applications. *Separation & Purification Reviews*, *46*(1), 62-80.

Qasem, N. A., Mohammed, R. H., & Lawal, D. U. (2021). Removal of heavy metal ions from wastewater: A comprehensive and critical review. *Npj Clean Water*, *4*(1), 1-15.

Ramli, N. H., Zakaria, C. S., Sueb, M. M., Abd Rahman, S., & Hisham, N. B. (2020). Elucidation of flux decline phenomenon in ultrafiltration of polydisperse silica solution. In *IOP Conference Series: Materials Science and Engineering* (Vol. 736, No. 2, p. 022097). IOP Publishing.

Rani, S. L. S., & Kumar, R. V. (2021). Insights on applications of low-cost ceramic membranes in wastewater treatment: A mini-review. *Case Studies in Chemical and Environmental Engineering*, 100149.

Rastgar, M., Shakeri, A., Bozorg, A., Salehi, H., & Saadattalab, V. (2017). Impact of nanoparticles surface characteristics on pore structure and performance of forward osmosis membranes. *Desalination*, *421*, 179-189.

Sankaranarayanan, S., Likozar, B., & Navia, R. (2019). Real-time particle size analysis using the focused beam reflectance measurement probe for in situ fabrication of polyacrylamide–filler composite materials. *Scientific reports*, *9*(1), 1-12.

Shokri, E., & Yegani, R. (2017). Novel adsorptive mixed matrix membrane by incorporating modified nanoclay with amino acid for removal of arsenic from water. *Journal of Water and Environmental Nanotechnology*, *2*(2), 88-95.

Shokri, E., Shahed, E., Hermani, M., & Etemadi, H. (2021). Towards enhanced fouling resistance of PVC ultrafiltration membrane using modified montmorillonite with folic acid. *Applied Clay Science*, *200*, 105906.

Simona, C., Raluca, I., Anita-Laura, R., Andrei, S., Raluca, S., Bogdan, T., ... & Dan, D. (2017). Synthesis, characterization and efficiency of new organically modified montmorillonite polyethersulfone membranes for removal of zinc ions from wastewasters. *Applied Clay Science*, *137*, 135-142.

Singh, S., Varghese, A. M., Reddy, K. S. K., Romanos, G. E., & Karanikolos, G. N. (2021). Polysulfone mixed-matrix membranes comprising poly (ethylene glycol)-grafted carbon nanotubes: mechanical properties and CO2 separation performance. *Industrial & Engineering Chemistry Research*, *60*(30), 11289-11308.

Sonawane, S., Thakur, P., Sonawane, S. H., & Bhanvase, B. A. (2021). Nanomaterials for membrane synthesis: Introduction, mechanism,a nd challenges for wastewater treatment. *Handbook of Nanomaterials for Wastewater Treatment*, 537-553.

Subasi, Y., & Cicek, B. (2017). Recent advances in hydrophilic modification of PVDF ultrafiltration membranes–a review: part I. *Membrane Technology*, *2017*(10), 7-12.

Tan, X., & Rodrigue, D. (2019). A review on porous polymeric membrane preparation. Part I: production techniques with polysulfone and poly (vinylidene fluoride). *Polymers*, *11*(7), 1160.

Tan, X., Liu, F., Hu, L., Reed, A. H., Furukawa, Y., & Zhang, G. (2017). Evaluation of the particle sizes of four clay minerals. *Applied Clay Science*, *135*, 313-324.

Tatulian, S. A. (2013). Structural characterization of membrane proteins and peptides by FTIR and ATR-FTIR spectroscopy. In *Lipid-protein interactions* (pp. 177-218). Humana Press, Totowa, NJ.

Uddin, F. (2018). *Montmorillonite: An introduction to properties and utilization* (pp. 3-23). London, UK: IntechOpen.

Vadgama, V. S., Vyas, R. P., Jogiya, B. V., & Joshi, M. J. (2017, May). Synthesis and characterization of CdO nano particles by the sol-gel method. In *AIP Conference Proceedings* (Vol. 1837, No. 1, p. 040016). AIP Publishing LLC.

Vinoba, M., Bhagiyalakshmi, M., Alqaheem, Y., Alomair, A. A., Pérez, A., & Rana, M. S. (2017). Recent progress of fillers in mixed matrix membranes for CO2 separation: A review. *Separation and Purification Technology*, *188*, 431-450.

Virtanen, T., Rudolph, G., Lopatina, A., Al-Rudainy, B., Schagerlöf, H., Puro, L., ... & Lipnizki, F. (2020). Analysis of membrane fouling by Brunauer-Emmet-Teller nitrogen adsorption/desorption technique. *Scientific reports*, *10*(1), 1-10.

Vu, M. T., Monsalve-Bravo, G. M., Lin, R., Li, M., Bhatia, S. K., & Smart, S. (2021). Mitigating the Agglomeration of Nanofiller in a Mixed Matrix Membrane by Incorporating an Interface Agent. *Membranes*, *11*(5), 328.

Won, J., Park, J., Kim, J., & Jang, J. (2021). Impact of Particle Sizes, Mineralogy and Pore Fluid Chemistry on the Plasticity of Clayey Soils. *Sustainability*, *13*(21), 11741.

Yaseen, M., Farooq, M. U., Ahmad, W., & Subhan, F. (2021). Fabrication of rGO-CuO and/or Ag2O nanoparticles incorporated polyvinyl acetate based mixed matrix membranes for the removal of Cr6+ from anti-corrosive paint industrial wastewater. *Journal of Environmental Chemical Engineering*, *9*(2), 105151.

Zuo, W., Yu, Y., & Huang, H. (2021). Making waves: Microbe-photocatalyst hybrids may provide new opportunities for treating heavy metal polluted wastewater. *Water Research*, *195*, 116984.

APPENDIX

Particle size distribution of MMT powder

Table 1: Particle size distribution numerical values for MMT powder

Sample	Particle size range (µm)	D_{10} (µm)	D_{50} (µm)	D_{90} (µm)	Mean diameter (µm)	Mode diameter (µm)
MMT	1.60 - 45.0	3.74	12.08	24.30	13.21	16.0

Water Uptake

Table 2: Numerical data for water uptake of pristine, 0.5MMM, 1.0MMM and 1.5MMM membranes

Membrane	Condition	Average weight (g)	Water uptake (%)
Pristine PSf	Dry	0.00750	36.67
	Wet	0.01025	
0.5 MMM	Dry	0.00775	74.19
	Wet	0.01350	
1.0 MMM	Dry	0.00825	81.82
	Wet	0.01500	
1.5 MMM	Dry	0.00825	87.88
	Wet	0.01550	

For pristine PSf membrane,

$$\text{Water uptake} = \frac{(0.01025\text{-}0.00750)\text{g}}{0.00750\text{g}} \times 100\% = 36.67\%$$

Pure Water Flux

Table 3: Numerical data for pure water flux of pristine, 0.5MMM, 1.0MMM and 1.5MMM membranes

Membrane	Time taken to fill in 5mL (s)	Pure water flux (L/m^2.h)
Pristine	14.53	1287.75
0.5 MMM	10.16	1841.64
1.0 MMM	7.35	2545.72
1.5 MMM	7.07	2646.54

For pristine PSf membrane,

$$J = \frac{0.005L}{\left(0.000962m^2 \times 14.53s \times \frac{1h}{3600s}\right)} = 1287.75 L/m^2.h$$

Surface Porosity

Table 4: Numerical data for surface porosity of pristine, 0.5MMM, 1.0MMM and 1.5MMM membranes

Membrane	W_{wet} (g)	W_{dry} (g)	Surface porosity (%)
Pristine	0.01025	0.00750	4.0838
0.5 MMM	0.01350	0.00775	8.5388
1.0 MMM	0.01500	0.00825	10.0238
1.5 MMM	0.01550	0.00825	10.7663

For pristine PSf membrane,

$$P = \frac{(0.01025 - 0.00750g)}{(1 \times 10^6 g/m^3)(0.000962m^2)(0.00007m)} \times 100\% = 4.0838\%$$

Heavy Metal Rejection

Table 5: Numerical data for cadmium rejection of pristine, 0.5MMM, 1.0MMM and 1.5MMM membranes

Membrane	Concentration (ppm)		Rejection (%)	Time taken to fill 5mL (s)	Permeate flux ($L/m^2.h$)
	Standard	Permeate			
Pristine	0.5051	0.4801	4.95	16.48	1135.38
0.5MMM	0.5051	0.5049	0.04	10.41	1797.41
1.0MMM	0.5051	0.4892	3.15	9.38	1994.78
1.5MMM	0.5051	0.5051	0	8.82	2121.43

For pristine PSf membrane,

$$R = \frac{(0.5051\text{-}0.4801)\text{ppm}}{0.5051\text{ppm}} \times 100\% = 4.95\%$$

$$\text{Permeate flux} = \frac{0.005\text{L}}{\left(0.000962\text{m}^2 \times 16.48\text{s} \times \frac{1\text{h}}{3600\text{s}}\right)} = 1135.38\text{L/m}^2\text{.h}$$

Table 6: Numerical data for lead rejection of pristine, 0.5MMM, 1.0MMM and 1.5MMM membranes

Membrane	Concentration (ppm)		Rejection (%)	Time taken to fill 5mL (s)	Permeate flux ($L/m^2.h$)
	Standard	Permeate			
Pristine	4.9536	4.4454	10.26	16.51	1133.31
0.5MMM	4.9536	4.2422	14.36	11.11	1684.16
1.0MMM	4.9536	4.2960	13.28	10.90	1716.61
1.5MMM	4.9536	4.7025	5.07	9.42	1986.31

For pristine PSf membrane,

$$\text{Rejection} = \frac{(4.9536\text{-}4.4454)\text{ppm}}{4.9536\text{ppm}} \times 100\% = 10.26\%$$

$$\text{Permeate flux}=\frac{0.005\text{L}}{\left(0.000962\text{m}^2\times 16.51\text{s}\times\frac{1\text{h}}{3600\text{s}}\right)}=1133.31\text{L/m}^2\text{.h}$$